Marine Micropaleontology 152 (2019) 101729

Contents lists available at ScienceDirect

Marine Micropaleontology

journal homepage: www.elsevier.com/locate/marmicro

Coupling plankton - sediment trap - surface sediment coccolithophore regime in the North Aegean Sea (NE Mediterranean)

E. Skampa[a,*], M.V. Triantaphyllou[a], M.D. Dimiza[a], A. Gogou[b], E. Malinverno[c], S. Stavrakakis[b], I.P. Panagiotopoulos[a,b], C. Parinos[b], K.-H. Baumann[d]

[a] National and Kapodistrian University of Athens, Faculty of Geology and Geoenvironment, Panepistimioupolis, 15784, Athens, Greece
[b] Hellenic Centre for Marine Research, Institute of Oceanography, PO Box 712, 19013 Anavyssos, Greece
[c] University of Milano-Bicocca, Department of Earth and Environmental Sciences, Italy
[d] University of Bremen, Department of Geosciences, PO Box 33 04 40, 28334 Bremen, Germany

A B S T R A C T

Quantitative coccolithophore analyses were performed on data of 2011–2015 dataset derived from the examination of plankton samples (until 100 m water depth), the sinking particulate matter (collected by a time series sediment trap) and surface and core sediments of the North Aegean Sea sampling site M2 (Athos Basin, NE Mediterranean). The aim was to achieve a better understanding of the potential modifications of the coccolithophore assemblage between the surface waters (plankton), the water column (sidocoenosis) and the underlying sediment (thanatocoenosis). Sediment trap calcareous nannoplankton multiannual mean fluxes (20×10^8 coccoliths $m^2\,day^{-1}$) documented similar values to the accumulation rates recorded in the surface sediment (23.6×10^8 coccoliths $m^{-2}\,day^{-1}$), whereas within the last 500 years the rates have ranged from 2.19×10^8 to 5.4×10^8 coccoliths $m^{-2}\,day^{-1}$. The dominant species in all sampling types was *Emiliania huxleyi*, reaching in some cases striking relative abundances of 85–90%. Morphometric analyses on *E. huxleyi* coccoliths documented the presence of a lightly calcified morphotype in the water column and sediment trap samples in addition to the seasonal occurrence of heavier calcified *E. huxleyi* coccoliths, indicating enhanced Black Sea water inflows during May 2011, February 2015 and October 2015. However, such a signal was not preserved in the surface sediment assemblage mostly due to processes of diagenetic calcite overgrowth. Notably, *Florisphaera profunda* was not included in the upper water column plankton assemblage but in the sediment traps and surface sediments. Thus, it is presumed to flourish in nutrient-enriched layers below the sampled 100 m water column depth. Several fragile Syracosphaeraceae and holococcolithophore species and the delicate *Algirosphaera robusta* were not present in the sinking assemblage or on the seafloor; however, the main features of the living assemblages were generally preserved. The recorded high relative abundances of *E. huxleyi* (~60%) in the sediment were in accordance with positive North Atlantic Oscillation (NAO) shifts during recent production of dense water masses in the North Aegean.

1. Introduction

Coccolithophores as a major photosynthetic and calcifying unicellular phytoplankton group play a key role in the biochemical cycles and the global climate system because of their contribution to inorganic carbon transportation to the ocean floor and, consequently, to the sedimentary archive (e.g., Westbroek et al., 1993; Rost and Riebesell, 2004; Beaufort et al., 2011). In addition, they represent reliable indicators of environmental conditions since they directly depend on surface water temperature, salinity, nutrient concentration and availability of sunlight (Winter et al., 1994; Baumann et al., 2000). Changes in fossil coccolithophore assemblages that are recorded in marine sediments generally comprise a successful paleontological tool for the reconstruction of the paleoclimatic and paleoceanographic conditions in the geological past (e.g., Negri and Giunta, 2001; Triantaphyllou et al., 2009; Bolton et al., 2016; Gogou et al., 2016; Athanasiou et al., 2017). However, with a few exceptions, little is known about the transformation of living coccolithophore communities (biocoenoses) into coccolith assemblages (taphocoenoses) within the underlying sediments (e.g., Baumann et al., 2000; Andruleit et al., 2004; Boeckel and Baumann, 2008; Saavedra-Pellitero and Baumann, 2015); the aforementioned studies have described reasonably good correlations between the occurrence and distribution of coccoliths in surface sediment samples and the corresponding overlying plankton samples. Therefore, in order to improve our knowledge for the application of coccolithophores as a proxy it is crucial to regard not just the ecology, biology, biogeography and oceanographic significance of extant coccolithophores but also the taphonomical processes that may alter the assemblages during sedimentation through the water column and during burial in the seafloor (e.g., Andruleit et al., 2004).

In the oligotrophic waters of the Eastern Mediterranean Sea, the high seasonality of parameters such as sea surface temperature, solar radiation, nutrient concentration and circulation of surface water masses affect coccolithophore abundance and productivity with a high

* Corresponding author.
E-mail address: elskampa@geol.uoa.gr (E. Skampa).

https://doi.org/10.1016/j.marmicro.2019.03.001
Received 18 May 2018; Received in revised form 24 November 2018; Accepted 2 March 2019
Available online 19 March 2019
0377-8398/

species number and strong seasonal variability (Kleijne, 1991; Triantaphyllou et al., 2002, 2004; Malinverno et al., 2003, 2009, 2014; Ignatiades et al., 2009; Dimiza et al., 2008, 2015). The North Aegean Sea (NE Mediterranean) displays less oligotrophic characteristics during the highest productivity spring period (Ignatiades et al., 2002; Zervoudaki et al., 2011), while coccolithophores constitute an important phytoplankton group (e.g., Dimiza et al., 2015; Karatsolis et al., 2017). However, a better knowledge regarding the linkage of the North Aegean extant coccolithophore communities to the fossil assemblages and their response to the prevalent environmental regimes may provide more reliable reconstructions of past environments, since this particular area is ideal for reconstructions of past climatic changes due to its unique physical and geographic configuration (e.g., Gogou et al., 2016).

The present study uses new data from the North Aegean sampling site M2, provided by sediment trap time series, surface sediments combined with plankton samples (Dimiza et al., 2015) and a sediment core record (Gogou et al., 2016), in order to make a synthesis of the coccolithophores' regime in the photic zone and assess their contribution to the sinking matter towards the seafloor, their preservation as surface sediment particles and, finally, their impact on the sedimentary record. The composition of the coccolithophore assemblage as well as the detailed morphometric analyses of the *Emiliania huxleyi* coccolith calcification degree are used to trace the origin of the various morphotypes of this species and support the detection of different water masses in the North Aegean Sea water column. The understanding of the modifications between the plankton vs. the exported assemblages and the sediment taphocoenoses can further establish coccolithophores as valuable proxies for the investigation of water column response to paleoceanographic changes (e.g., dense water formation events) in the North Aegean and analogous oceanic sites of deep water formation.

2. Oceanographic setting and coccolithophore assemblage composition

The Aegean Sea (NE Mediterranean) exhibits complicated physical and geographic configurations, while it communicates in the northeast with the Black and Marmara seas through the Dardanelles Straits and in the south with the open Eastern Mediterranean Sea (Levantine) through the Cretan Straits. It is located in a transition zone between temperate and semiarid climate conditions with an average annual sea surface temperature (SST) of 18.2 °C (e.g., Parker et al., 1995). Low-salinity (24–28 psu) surface Black Sea water (BSW; < 70 m depth) outflows from Dardanelles and is driven along the eastern coast of Greece until it reaches the southwestern Aegean (Lykousis et al., 2002). During winter, BSW tends to flow northwest of Limnos Island filling the northernmost part of the Aegean before moving westwards (Lascaratos, 1992) (Fig. 1); in summer, the strong northerly winds blowing over the Aegean deflect the BSW to some extent south of Limnos. BSW inflow rates show strong seasonal and interannual variability, reaching a maximum during mid to late summer and a minimum during winter (Zervakis et al., 2000). Salty (>39 psu) Levantine surface water (LSW) occupies the upper water column in the absence of BSW, while Levantine intermediate water (LIW; 14–15 °C, 38.8–39.1 psu) extends to a depth of up to ~400 m below the BSW/LSW. These Levantine water masses flow northwards along the eastern Aegean until they meet the outflowing surficial BSW (e.g., Zervakis et al., 2004). The low-density BSW surface layer spreading during winter acts as an insulating lid that impedes air–sea interactions, resulting in the stratification of the water column and hindering dense water formation over the area it covers in the North Aegean (Zervakis et al., 2000, 2004; Velaoras and Lascaratos, 2010; Androulidakis et al., 2012; Velaoras et al., 2013). Relatively recently deep-water formation has been reported for the North Aegean, under the influence of anomalously cold winters, known as the Eastern Mediterranean transient (EMT; Theocharis et al., 1999, 2014), which has been proven to ventilate the water column of the basin from the surface down to 650 m (Velaoras et al., 2017).

In the euphotic zone of the North Aegean (0–100 m), the nitrate concentrations vary from 0.05 to 1.6 μM with the phosphate values ranging from 0.02 to 0.08 μM (Lykousis et al., 2002; Souvermezoglou et al., 2014). Additional data for the NE Aegean Basin (Table 1a; Chl-a, temperature, salinity, oxygen, nutrients) evidence that the BSW surface layer (with salinities of 34–36 psu) occupies the upper 20 m of the water column, while higher nutrient concentrations and phytoplankton biomass have been recorded during a spring (March) sampling (nitrates: 0.05–0.07 μM, phosphates:74–14.56 nM; Karatsolis et al., 2017; Lagaria et al., 2017). In addition, Souvermezoglou and Krasakopoulou (2002) have detected the North Aegean nutricline at ~150 m depth.

This oligotrophic region may display mesotrophic characteristics during the high-productivity spring period, influenced by the BSW influx, with chlorophyll-a (Chl-a) reaching concentrations of 1 $\mu g\,l^{-1}$ (Ignatiades et al., 2002; Zervoudaki et al., 2011; Lagaria et al., 2013; Malinverno et al., 2016). Despite the presence of the surface BSW layer, Chl-a values are lower during fall (~0.2 $\mu g\,l^{-1}$), making the basin an oligotrophic area (Ignatiades et al., 2002; Lagaria et al., 2013, 2017). The surface Chl-a concentrations measured by satellite (NASA SeaWiFS data, available at http://disc.sci.gsfc.nasa.gov/techlab/giovanni) range seasonally from 0.1 to 1.31 $\mu g\,l^{-1}$. Low values are demonstrated during summer and increased ones in the fall-winter period, while they reach a maximum from late winter to early spring (Fig. 2a). The sea surface productivity cycle, as derived from satellite-sensed Chl-a, displays a pattern that is opposite to that of SST maxima (Fig. 2a). The SST values (Table 1a; NASA SeaWiFS data, available at http://disc.sci.gsfc.nasa.gov/techlab/giovanni;Acker and Leptoukh, 2007) subdivide the annual cycle in two periods, i.e., the warm from May to November and the cold in-between December and April (values up to 27.9 and 19.3 °C respectively; Fig. 2a). The annual variation of precipitation is anticorrelated with the SST pattern (see Fig. 2a). During 2011–15, the rainy season in the North Aegean took place from November to March, with the longest and more intense rainy season occurring during fall 2014-winter 2015 (Fig. 2a). Potential nutrient input from precipitation and discharges of several rivers, supplying the North Aegean Basin with land-derived organic matter, especially during winter time (Poulos et al., 1997; Roussakis et al., 2004), may enhance marine productivity.

Coccolithophore plankton assemblages in the North Aegean region are dominated by *E. huxleyi* and several Syracosphaeraceae species (Dimiza et al., 2015; Karatsolis et al., 2017); however the two distinct water masses in the North Aegean, i.e., BSW and LIW, are differentiated by their coccolithophore assemblage composition. The BSW mass in the surface is entirely dominated by the species *E. huxleyi* (e.g., Triantaphyllou et al., 2014), with lightly calcified morphotypes (Karatsolis et al., 2017) being present in the inflowing BSW throughout the year. An intense decrease of this species abundance towards the mid photic zone marks the presence of the LIW layer. Although several species of *Syracosphaera* contribute significantly to the coccolithophore communities, the presence of the LIW is primarily reflected by the prevalence of *Umbellosphaera tenuis, Syracosphaera pulchra* and holococcolithophores in the occurring assemblage (Dimiza et al., 2015; Karatsolis et al., 2017). During limited inflows of BSW, especially during the winter time, the nutrient-enriched North Aegean water column is dominated again by *E. huxleyi,* but displaying that time the characteristic overcalcified morphotypes of the cold season (Triantaphyllou et al., 2010). A recent fossil record from the same geographic location (Gogou et al., 2016) reveals the dominance of both *E. huxleyi* and *Florisphaera profunda* with anticorrelating patterns.

3. Materials and methods

3.1. Plankton samples

Plankton samples from the Athos Basin of North Aegean (M2 sampling site, 40° 05.15′N, 24° 32.68′E; Fig. 1, Table 1a) were collected during January 2011 (3–100 m depth) and May 2011 (5–90 m depth)

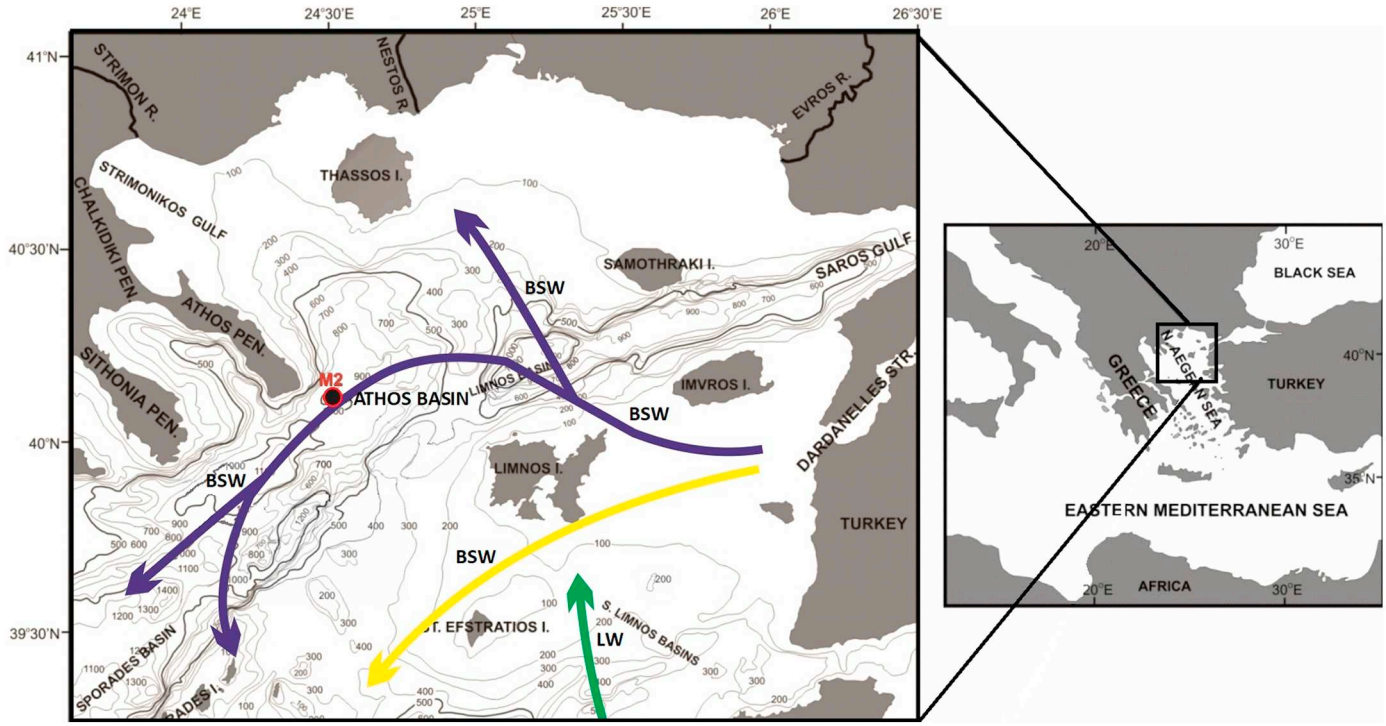

Fig. 1. Plankton, sediment trap and surface sediment sampling site location (M2), in the North Aegean Sea. Bathymetry is according to Roussakis et al. (2004), arrows show the main patterns of sea water surface circulation. BSW: Black Sea Water main pathways during winter (blue) and additional pathway during summer (yellow), LW: Levantine Water (green). (For interpretation of the references to colour in this figure legend, the reader is referred to the web version of this article.)

Table 1a
M2 site location details for the investigated plankton sampling at the North Aegean Sea and available oceanographic data. Additional data from a neighboring site (AMT-2; Karatsolis et al., 2017; Lagaria et al., 2017) are also presented.

Station code	AMT-2*	AMT-2*	M2**	M2***
Latitude (°N)	39° 15.00′	39° 15.00′	40° 05.15′	40° 05.15′
Longitude (°E)	25° 26.76′	25° 26.76′	24° 32.68′	24° 32.68′
Sampling type	rosette	rosette	rosette	rosette
Date	October 2013	March 2014	January 2011	May 2011

Depth (m)	0–20	30–75	0–20	30–75	3	20	50	75	100	5 30	60 90
Temperature (°C)	19.7–21.12	16.84–19.8	12.56–13.34	3.82–15.15	15.91	16	16.31	16.48	16.7	17.27	no data
Salinity (psu)	34.15–35.53	37.05–39.07	33.71–36.43	37.69–38.84	38.35	38.38	38.51	38.62	38.76	no data	
Oxygen (ml l^{-1})	4.53–4.87	5.12–5.46	5.92–6.1	5.2–5.66	no data	no data	no data	no data	no data		
Chl-a (μg l^{-1})	0.12–0.13	0.14–0.22	0.22–0.41	0.13–0.48	0.1	0.156	0.196	0.059	0.099	0.9	no data
PO_4 (nM)	15–30.11	15–27	74–114.56	75.67–229.56	no data	no data	no data	no data	no data	no data	
NO_3 + NO_2 (μM)	0.17–0.43	0.17–0.41	0.05–0.07	0.07–0.75	no data	no data	no data	no data	no data		

* Karatsolis et al. (2017), Lagaria et al. (2017).
** Dimiza et al. (2015).
*** Analyses and visualizations used in this study were produced with the Giovanni online data system, developed and maintained by the NASA GES DISC.

on board the R/V Aegaeo. Temperature and salinity data were obtained during the January 2011 sampling period (Table 1a). For each plankton sample, 2 l of seawater were filtered on Whatman cellulose nitrate filters (47 mm diameter, 0.45 μm pore size), which were rinsed with about 2 ml of buffered distilled water (pH > 8) to remove salt. A piece of each filter approximately 8 × 8 mm^2 was attached to a copper electron microscope stub, using a double-sided adhesive tape and coated with gold. The filters were examined in a JEOL JSM 6360 scanning electron microscope and all the individual coccospheres occurring on the examined filter area were identified and counted at 1200× to calculate coccolithophore absolute (cells l^{-1}) and relative abundances (Dimiza et al., 2015).

3.2. Sediment trap

A time series sediment trap (PPS3/3 Technicap, 0.125 m^2 collecting area) was deployed at 500 m depth in the M2 site of Athos Basin (Fig. 1, Table 1b) for the estimation of export fluxes during the time-intervals January 2011–December 2011 and October 2014–November 2015. Upon recovery of the traps, samples were fixed (with a 5% formaldehyde solution mixed with filtered seawater and buffered with sodium borate; Stavrakakis et al., 2000) and stored in the dark at 2 °C, until further processing. Swimmers were removed by hand picking under a stereoscope and sub-sampling was undertaken using a peristaltic pump (Perimatic Premier, Jencons). The total mass flux, organic

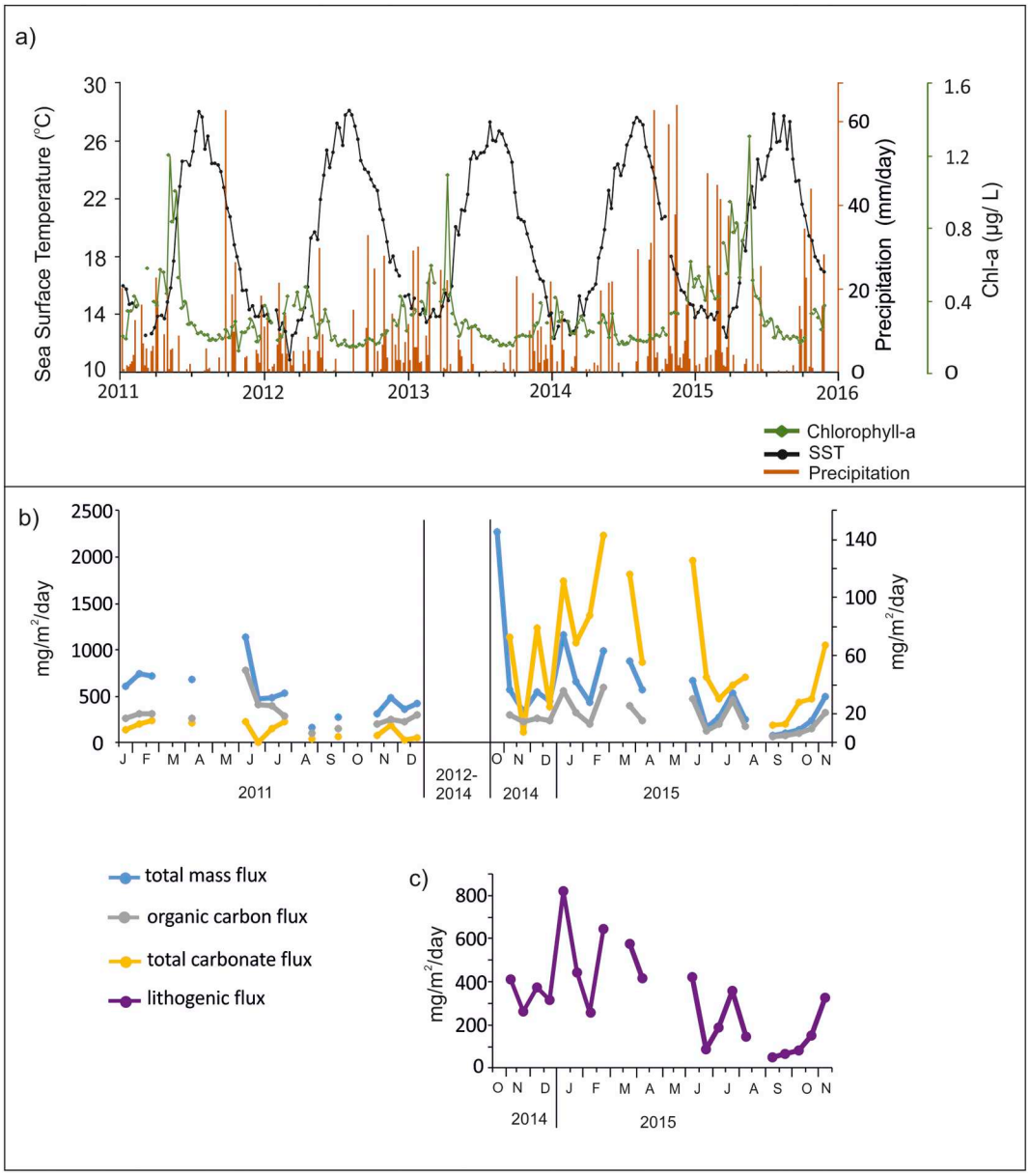

Fig. 2. a. Oceanographic and satellite-derived data in the study area: a) SST, Chlorophyll -a and precipitation during the study interval, all satellite data are obtained at http://disc.sci.gsfc.nasa.gov/techlab/giovanni/, (analyses and visualizations used in this study were produced with the Giovanni online data system, developed and maintained by the NASA GES DISC.), b. total mass and biogenic fluxes at the 500 m depth, derived from the sediment trap, c. lithogenic flux at the 500 m depth, derived from the sediment trap.

carbon contents, carbonate content and lithogenic fraction (quartz, aluminosilicates, heavy minerals) were calculated as in Stavrakakis et al. (2000) and Stavrakakis et al. (2013). For the coccolithophore analysis, each sub-sample was split into 10 equal fractions by the use of a McLane rotary wet splitter, with $<4\%$ deviation between aliquots. A vacuum pump was used to filter the produced aliquots onto Millipore cellulose filters (47 mm diameter, 0.45 µm pore size), which were rinsed with buffered distilled water (pH > 8), dried in an oven and stored in plastic petri dishes. For the coccolith sample preparation aliquots were further split, organic material was oxidized following Bairbakhish et al. (1999) and each sub-sample was sieved over a 32 µm mesh sieve. For each sediment trap sample, two different slides were prepared mounting a portion of filter from coccosphere and coccolith splits respectively, and were analyzed using a polarized light optical Leica DMLSP microscope (LM) at 1250×. Approximately 20 mm^2 were investigated to determine total coccosphere fluxes and coccospheres per species, whereas total coccoliths and coccoliths per species were counted within an area of 2 mm^2 (e.g., Ziveri et al., 1999; Triantaphyllou et al., 2004). Calcareous nannoplankton fluxes were calculated via extrapolation to the entire effective filtration area and total sample, duration days and trap aperture area, according to the following equation (Ziveri et al., 1999): $F = N \times Af \times S/af \times Ast \times T$, where F = flux (specimens $m^{-2}\,day^{-1}$), N = number of counted specimens, Af = effective filtration area (mm^2), S = split factor, af = investigated filtration area (mm^2), Ast = sediment trap aperture area (m^2), T = sample collecting time (days). Coccosphere units were converted to coccolith numbers according to Boeckel and Baumann (2008).

3.3. Sediment record

A 48-cm-long core was, acquired from the M2 site in 2011 using a multicorer system (Athos Basin, 1018 m depth; Fig. 1, Table 1b). Sediments consisted mainly of olive gray to grayish olive homogeneous mud, with high contents of silt (25–45% dw) and clay (40–60% dw).

Table 1b
M2 site location details for the investigated sediment trap, core and surface sediment sampling in the North Aegean Sea.

M2 Site details		
Location	Coordinates	Water column depth (m)
M2 site (Athos basin, North Aegean Sea)	40° 05.15′N, 24° 32.68′E	1018
Multicore/Surface sediment		
cruise-ship	*core code-type*	*core length (cm)*
MEDECOS II-R/V Aegaeo	M2-multicore	48
Sediment trap		
Sediment trap code		*depth from sea surface*
AM2		500 m
Sample	*Start sampling date*	*Sampling duration*
AM2-A1	13/01/2011	19
AM2-A2	01/02/2011	15
AM2-A3	15/02/2011	14
AM2-A6	01/04/2011	15
AM3-A1	07/05/2011	25
AM3-A2	01/06/2011	15
AM3-A3	16/06/2011	15
AM3-A4	01/07/2011	15
AM3-A5	16/07/2011	16
AM3-A6	01/08/2011	31
AM3-A7	01/09/2011	30
AM3-A9	01/11/2011	15
AM3-A10	16/11/2011	15
AM3-A11	01/12/2011	15
AM3-A12	16/12/2011	16
M2IA1	16/10/2014	16
M2IA2	01/11/2014	15
M2IA3	16/11/2014	15
M2IA4	01/12/2014	15
M2IA5	16/12/2014	16
M2IA6	01/01/2015	15
M2IA7	16/01/2015	16
M2IA8	01/02/2015	15
M2IA9	16/02/2015	13
M2IA11	16/03/2015	16
M2IA12	01/04/2015	15
M2IIA1	01/06/2015	15
M2IIA2	16/06/2015	15
M2IIA3	01/07/2015	15
M2IIA4	16/07/2015	16
M2IIA5	01/08/2015	15
M2IIA7	01/09/2015	15
M2IIA8	16/09/2015	15
M2IIA9	01/10/2015	15
M2IIA10	16/10/2015	15
M2IIA11	01/11/2015	15

The core stratigraphy was based on a combination of ^{210}Pb measurements and accelerator mass spectrometry ^{14}C dates, revealing a decadal to multi-decadal high-resolution record for the last 1500 years (Gogou et al., 2016). The coccolithophore relative abundances in the upper 29 cm (the last 500 years according to the age model of Gogou et al., 2016) of the core were used in the present study to compare the photic zone assemblage and the water column export flux with the fossil record. The surface sample (0–1 cm, corresponding to the 2000–2010 time interval) was further analyzed to determine the coccolithophore relative and absolute abundances and accumulation rates on the seabed. In order to oxidize the organic matter, a solution of 0.1 g dry surface sediment and 3 ml of buffered distilled water (pH > 8) was treated according to Bairbakhish et al. (1999). A split fraction was filtered onto a Millipore cellulose nitrate filter (47 mm diameter, 0.45 μm pore size) using a pump vacuum. Quantitative analysis of coccoliths was estimated using a polarized Leica DMLSP (LM) at 1250× by counting 300 specimens present within at least 3 fields of view (FOV); additionally, 7 more FOV were analyzed for the minor species. The absolute abundance was calculated as: N (Number of coccoliths g^{-1} sediment) = F × C × S/A × W, where F = filtration area (mm^2); C = number of counted coccoliths; S = split factor; A = counted area (mm^2); W = sediment weight (g). These values were used to determine coccolith accumulation rates (number of coccoliths $cm^{-2}\,year^{-1}$) as AR = Dc x DBD x SR, with Dc = coccolith density (number of coccoliths g^{-1}), DBD = dry bulk density and SR = sedimentation rate. Accumulation rate was converted to number of coccoliths $m^2\,day^{-1}$ in order to be compared with the sediment trap coccolith fluxes.

3.4. Morphometric analyses on Emiliania huxleyi coccoliths

To carry out morphometric analyses on *E. huxleyi* type A, coccoliths from all types of samples (i.e., plankton of May 2011, sediment trap of 2015 time series, surface sediment), a piece of each filter was attached to a copper electron microscope stub by a double-sided adhesive tape and afterwards coated with gold. Each sample was scanned in a JEOL JSM 6360 scanning electron microscope and 40 flat-lying *E. huxleyi* coccoliths in distal view (in total 650 coccoliths) were photographed at 10,000× and analyzed through the ImageJ software. A series of coccolith morphometric measurements were applied following the biometric approaches of Young et al. (2014), i.e., coccolith length (CL), coccolith width (CW), tube width and, finally, relative tube width (RTW = 2 × tube width/ CW), which is a dimensionless and size-independent parameter used to measure the degree of calcification variation. The lack of coccolith mass measurements prohibited the application of other calcification indices that might more accurately reflect the calcification variability in the coccolith distal shield (e.g., D'Amario et al., 2018).

A series of Pearson correlations were performed on the dataset (Table 2), while the SPSS (version 10.1) statistical software was used for the detection of any possible correlation between the RTW and environmental parameters.

4. Results

4.1. Plankton Samples: absolute densities and relative abundances

The highest absolute coccolithophore densities (Dimiza et al., 2015) occurred at 20 m depth during January 2011 (26×10^3 coccospheres l^{-1}) and at 5 m depth during May 2011 (396×10^3 coccospheres l^{-1}) (Fig. 3a). Mean coccosphere absolute abundance in the sampled water column revealed obviously increased values during May (119×10^3 cells l^{-1}) vs. January (19×10^3 cells l^{-1}; Fig. 4a), with an evident

Table 2
Correlations among the Relative Tube Width (RTW) calcification index and the available environmental parameters.

Correlations							
		SST	Total Mass Flux	Org C Flux	Carbonates Flux	Lithogenic Flux	Chl-a
RTW	Pearson Correlation	−0.230**	0.001	−0.070	−0.078	0.009	0.102*
	Sig. (2-tailed)	0.000	0.990	0.163	0.121	0.864	0.042
	N	400	400	400	400	400	400

** Correlation is significant at the 0.01 level (2-tailed).
* Correlation is significant at the 0.05 level (2-tailed).

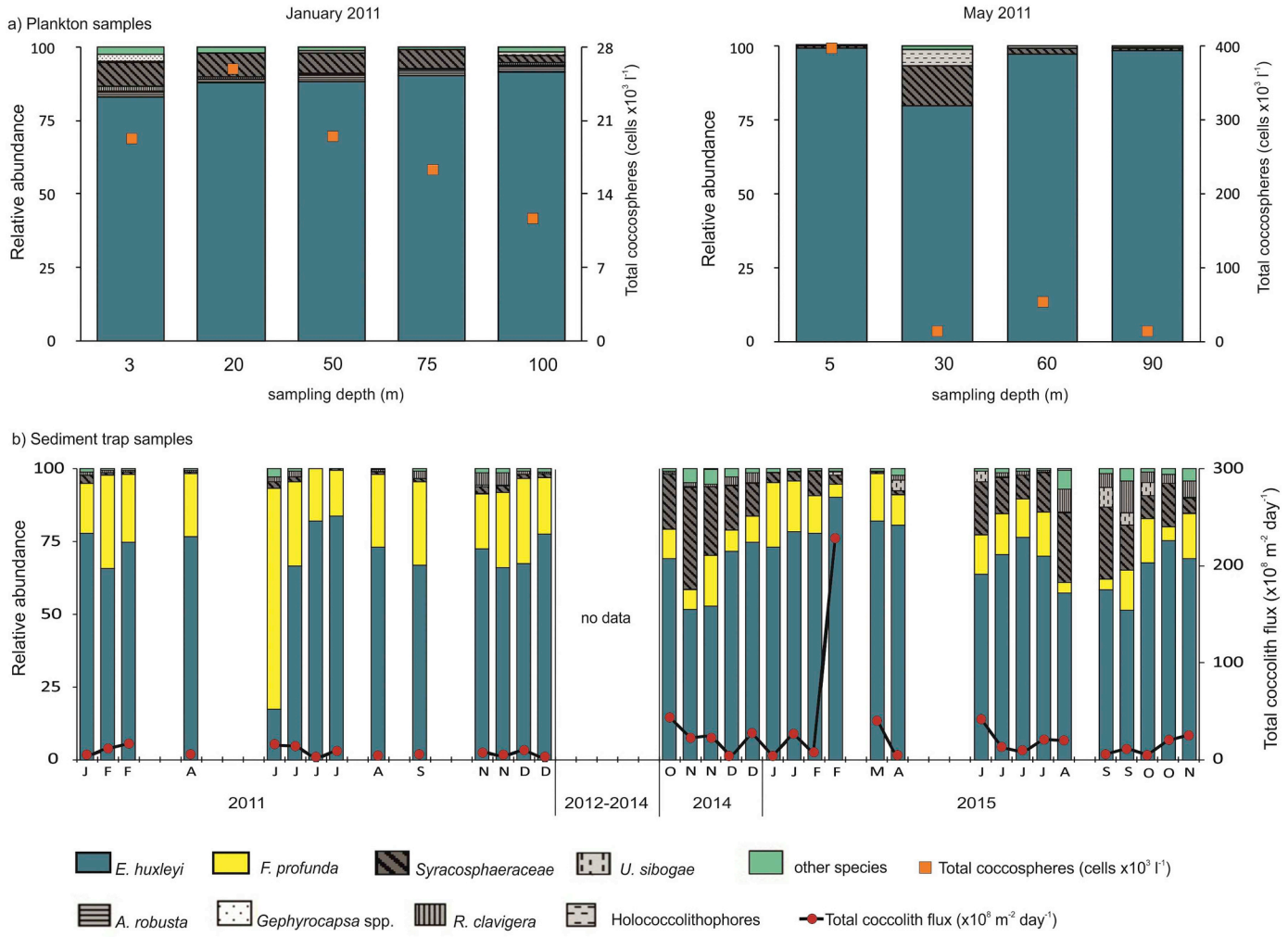

Fig. 3. a. Plankton samples absolute densities (total coccospheres l^{-1}) and species relative abundances for each sampling depth in January and May 2011, b. Sediment trap total coccolith export fluxes (coccoliths $m^{-2}\,day^{-1}$) and species relative abundances (January 2011–November 2015). For detailed species see Appendix 1.

mean annual relative abundance dominated by *E. huxleyi*, reaching >90%. Overall, *Emiliania huxleyi* type A was the dominant species (~80%) in all depths, followed by Syracosphaeraceae (mainly represented by *S. molischii*) (Fig. 3a). Other minor contributors were *Algirosphaera robusta*, *Rhabdosphaera clavigera, Gephyrocapsa* spp. and several holococcolithophore species, which mostly occurred at 3 m depth (Fig. 3a; Appendix 1). The holococcolithophore group consisted of *Algirosphaera robusta* HOL, *Corisphaera* sp. type A, *Helicosphaera carteri* HOL perforate type, *Helladosphaera cornifera*, *Poritectolithus poritectus*, *Syracolithus dalmaticus*, *S. halldalii* HOL var. *tuberosa* and *S. histrica* HOL, *Zygosphaera marsilii* (Appendix 1). In May 2011, the coccolithophore absolute densities were slightly exceeding those recorded in January 2011, with the exception of the 5 m depth level, where the values appeared remarkably higher (Fig. 3a) due to an extreme peak in *E. huxleyi* relative abundance (99%). Other species that contributed to the coccolithophore assemblage of May 2011 sampling were Syracosphaeraceae (mostly represented by *S. protrudens*) and holococcolithophore species, being mostly present at the 30 m depth level (Fig. 3a).

Interestingly, when the minor contributors in the plankton assemblage (mostly Syracosphaeraceae) were converted into coccoliths they presented increased values with a concomitant reduction of *E. huxleyi* to 80% in January 2011 and > 90% in May 2011 (Fig. 4a). The recorded mean annual relative abundance indicated a dominance of *E. huxleyi* of up to ~90%. Apparently, this synthetic assemblage frame is not totally realistic, since different species with different ecological preferences have been combined throughout the sampled water column (Andruleit et al., 2004).

4.2. Sediment trap samples: biogenic fluxes, calcareous nannoplankton export fluxes and assemblage composition

The total mass flux, estimated for the entire sampling period, reached a maximum value of 2272 mg $m^{-2}\,day^{-1}$ during late October 2014 (Fig. 2b). The total carbonate flux and total organic carbon flux followed the general trend of the total mass flux showing enhanced precipitation with the higher values being recorded during the low SST winter and early spring 2015 (Fig. 2a, b). The lithogenic flux (up to 70% of the total mass flux) followed the total mass flux pattern as well, with maxima appearing in winter-early spring 2015 (Fig. 2c) and the highest peak in early January 2015 (820 mg $m^{-2}\,day^{-1}$; Fig. 2c). The biogenic particle flux did not exceed 30% of the total mass flux, confirming that the origin of the major component of the mass flux is terrestrial, while it was associated with the precipitation peak (Fig. 2a).

The total calcareous nannoplankton flux in the North Aegean exhibited a moderate seasonal pattern during the time intervals from late January to December 2011 and late October 2014 to early November 2015 (Fig. 3b). In both investigated annual cycles, the higher coccolith fluxes were recorded during the cold period (late February 2011: 1.7×10^8 coccoliths $m^{-2}\,day^{-1}$; extreme peak in late February 2015: 229×10^8 coccoliths $m^{-2}\,day^{-1}$; Fig. 3b), followed by several

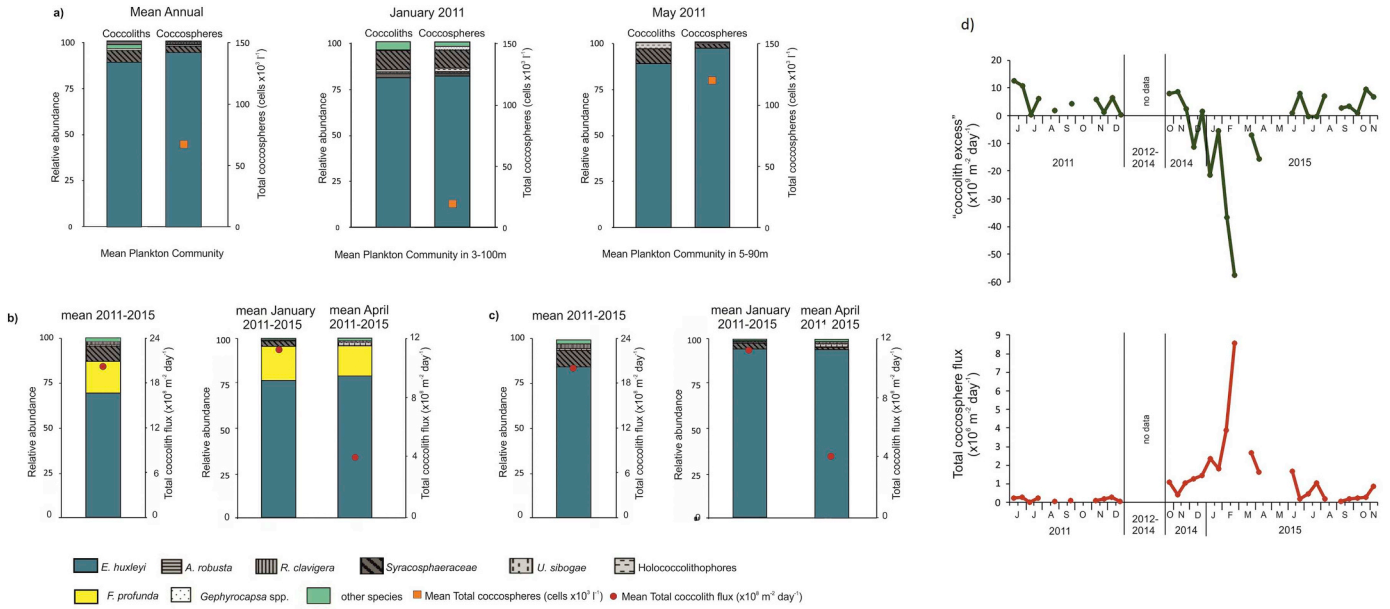

Fig. 4. a. Mean plankton community (total coccospheres l^{-1}), relative abundances and mean plankton community relative abundances of coccospheres converted to coccoliths (according to Boeckel and Baumann, 2008) of all sampling depths in January and May 2011 and mean annual values, b. Mean total coccolith flux and relative abundances of January and April 2011–2015 and mean annual values of 2011–2015, c. Mean total coccolith flux and relative abundances of January and April 2011–2015 and mean annual values of 2011–2015, excluding *F. profunda*, d. time-series plots of: "coccolith excess" flux (coccoliths m − 2 day − 1) showing the peaks in June 2011 and late October 2015 associated with re-sedimentation processes and excess minima in late February 2015; and total coccosphere flux (coccospheres m − 2 day − 1), where the prominent peak in late February 2015 represents high coccolithophore productivity during late winter-early spring.

fluctuations in the rest of the year. The total 2011–2015 mean flux was 20×10^8 coccoliths $m^2\,day^{-1}$ (Fig. 4b).

The seasonality of the coccosphere flux was similar to the total coccolith flux (Fig. 4d), whereas the calculated "coccolith excess" [coccolith flux minus the coccosphere flux $\times 10^3$] (Karageorgis et al., 2018) displayed an anticorrelated pattern to the coccosphere flux, with minimum values in winter-early spring 2015 (Fig. 4d).

Emiliania huxleyi was dominant during the whole investigated time period; the higher relative abundances, exceeding 90% of the species, were demonstrated mostly during the cold months in late February 2015 (Fig. 2b). *Florisphaera profunda* and Syracosphaeraceae (mostly *S. pulchra* and *S. mediterranea)* prevailed among the major species of the assemblage composition (Fig. 3b). Both had higher relative abundances during the warm period (May–November), coupled with *E. huxleyi* minima. Syracosphaeraceae displayed higher relative abundances during 2015 than 2011. Other species observed were *Umbilicosphaera sibogae* and *Rhabdosphaera clavigera*, which occurred in much lower abundances. Holococcolithophores (*Syracolithus dalmaticus*, *S. mediterranea* HOL *wettsteinii* type, *Helicosphaera carteri* HOL perforate type) contributed with very low percentages (average 2011–2015: 0.1%; Fig. 3b), while other minor species (see Appendix 1) were only sporadically present.

The January (2011–2015) mean relative abundances, plotted for comparison with the plankton samples (Fig. 4b), showed the prevalence of the two major species, *E. huxleyi* (up to 75%) and *F. profunda* (about 20%), and to a much lesser degree of Syracosphaeraceae. Since there were not any sediment trap data available for May, the data of April (2011 and 2015) were used for comparisons with the plankton data; these revealed the dominance of *E. huxleyi* (< 80%) over *F. profunda* and Syracosphaeraceae (Fig. 4b) with a minor contribution of *U. sibogae*. Mean export flux revealed increased values during January 2011–2015 (11.2×10^8 coccoliths $m^{-2}\,day^{-1}$; Fig. 4b), with the recorded mean annual relative abundance indicating a dominance of *E. huxleyi* of up to ~70%.

4.3. Surface sediment assemblages and relative abundance fluctuations in the fossil record

The surface sediment at the M2 sampling site displayed a mean coccolith AR of 23.6×10^8 coccoliths $m^{-2}\,day^{-1}$ (Fig. 5a), with *E. huxleyi* (12.9×10^8 coccoliths $m^{-2}\,day^{-1}$, 55%) clearly dominating over *F. profunda* (7.4×10^8 coccoliths $m^{-2}\,day^{-1}$, 32%). This pattern is rather similar to the one recorded during the cold period months in the sediment trap assemblages (Figs. 3, 4). Other minor species were present with abundances <3.5% (Appendix 1).

Throughout the 29 cm of the M2 core sediment (dated up to 1509), the prevalence of both *E. huxleyi* and *F. profunda* is the distinct feature of the coccolithophore assemblage; interestingly, the dominance of *E. huxleyi* over *F. profunda* demonstrated an obvious fluctuation pattern (Fig. 5c). The rest of the species contributed with negligible values (Appendix 1), with *Syracosphaera* spp. (3.5%) and *Rhabdosphaera* spp. (3%) being the most prominent.

ARs of total calcareous nannofossils were estimated for the last 500 years (Fig. 6a). The highest peak of the total ARs during this interval occurred in 1965 (5.4×10^8 coccoliths $m^{-2}\,day^{-1}$), followed by positive shifts at 1672, 1899, 1595, 1988 and 1921 (Fig. 6a). Even though the *E. huxleyi* AR followed the same pattern as the one of the total calcareous nannofossils, it can be noticed that the species major peak occurred in 1672 (3.79×10^8 coccoliths $m^{-2}\,day^{-1}$) followed by maxima at 1899, 1595, 1988, 1965 and 1921 (Fig. 6a).

4.4. Morphometric analyses on Emiliania huxleyi coccoliths

Morphometric analyses on the *E. huxleyi* coccoliths in the the plankton samples of May 2011 revealed RTW values ranging between 0.05 and 0.55 with a peak at ~0.10 in a unimodal distribution (Fig. 7a, Appendix 2). Coccolith RTW at the 5 m depth level was restricted to 0.05–0.15, at the 30 m depth level was mainly ~0.10, whereas at the 60 m and 90 m depth levels higher values (> 0.10) were noticed (Fig. 7a).

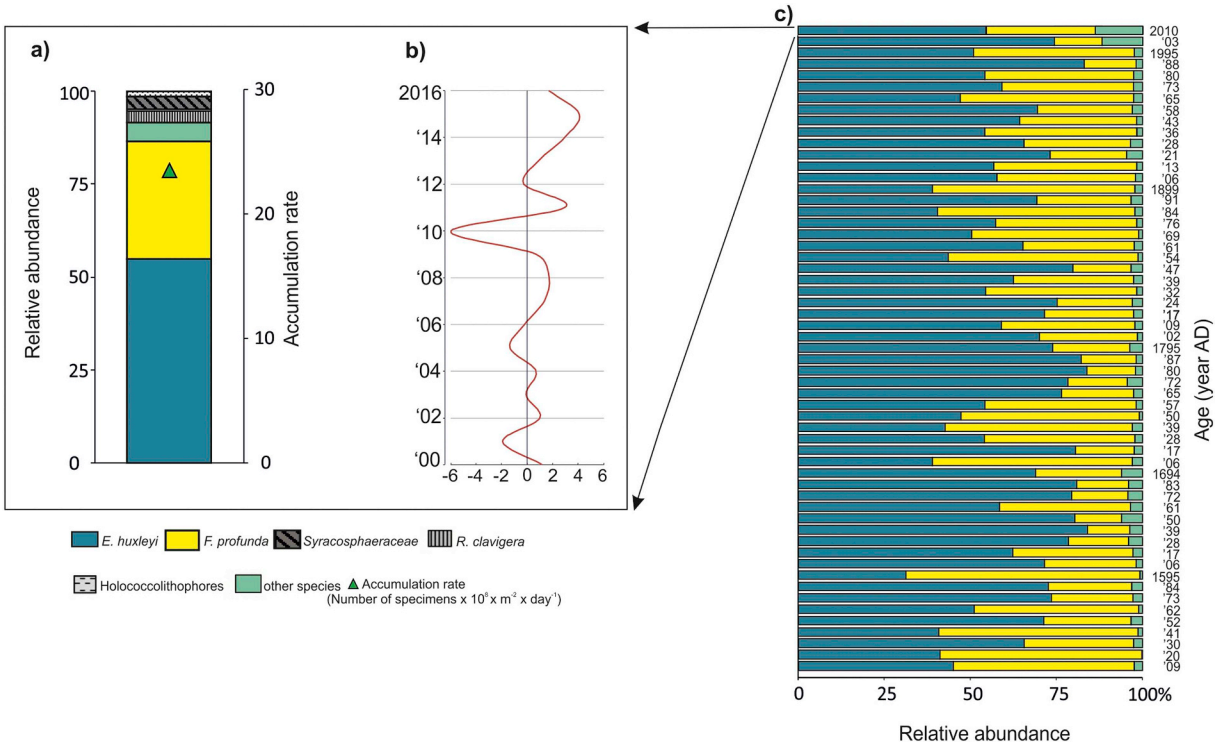

Fig. 5. a. Coccoliths accumulation rate and relative abundances in the surface sediment at M2 site, b. 2000–2016 NAO-index compiled from datasets of Hurrell et al. (2017) c. Coccolith relative abundances in the M2 multicore sediment record, for the last 500 yrs. (age model according to Gogou et al., 2016).

In the sediment trap samples, RTW followed a seasonal pattern (Fig. 7b), with specimens from the time interval May–November 2015, which corresponded to higher temperatures (up to 28 °C, Fig. 2a), displaying a bimodal distribution; peaks at ~0.10 and 0.30 (August and September, respectively), and 0.20 and 0.40 (October and November, respectively) were observed. During winter and early spring (~12–16 °C, Fig. 2a), the distribution was unimodal with values ranking between 0.10 and 0.40 with a higher frequency at ~0.30. Interestingly February values corresponding to temperature minima and high precipitation (Fig. 2a) displayed an unexpected second peak of low RTW (~0.10; Fig. 7b, Appendix 2).

Surface sediment coccolith biometry was unimodally displayed (Fig. 5c) with RTW ranking between 0.20 and 0.60 with a highest peak at 0.35.

Finally, the Pearson correlation analysis revealed that the two principal environmental factors that affected the RTW calcification parameter were the SST and Chl-a concentration (Table 2); calcification was negatively related to the SST but positively associated with the Chl-a concentration.

5. Discussion

5.1. Present-day coccolithophore assemblage: From plankton to sediment

The living coccolithophore community obtained from plankton sampling is under the influence of seasonal oceanographic changes and variation in seasonal productivity (e.g., Andruleit, 1997; Malinverno et al., 2003; Bonomo et al., 2012, 2018; Dimiza et al., 2008, 2015; Karatsolis et al., 2017), whereas sediment trap records may be affected by dissolution or selective destruction (e.g., Samtleben et al., 1995; Baumann et al., 2000; Andruleit et al., 2004). A secure way to overcome these methodological complications is the combination of data from both samplings in order to get a more realistic image of the species composition in the euphotic zone and the seasonal species oscillations in the water column.

Present data show that particularly *E. huxleyi* prevails in the plankton samples with the subordinate presence of Syracosphaeraceae. *E. huxleyi*, well known for its quick response to nutrient enrichment even in oligotrophic areas, such as the Eastern Mediterranean (Kleijne, 1991; Dimiza et al., 2008, 2015), occurs in high relative abundances in the current plankton (~90%) and sediment trap samples (~70%), especially during the winter-spring period (December to April; Figs. 3, 4a, b) that corresponds to the lowest temperatures and maximum precipitation and Chl-a concentration (Fig. 2a), and the associated increase in the nutrient supply of the photic zone (nitrates up to 0.75 μM; Table 1a; Karatsolis et al., 2017; Lagaria et al., 2017).

Yet, the absence of *F. profunda* in the sampled North Aegean water column (Figs. 3a, 4a) is quite striking, compared to its noticeable contribution to the sediment trap calcareous nannoplankton assemblage (Figs. 3b, 4b) and the sedimentary record (Fig. 5). *Florisphaera profunda*, which flourishes in the nutrient-rich deep photic zone (e.g., Molfino and McIntyre, 1990; Winter et al., 1994), should thrive below the sampled 100 m water layer (following the nutricline down to ~150 m; Souvermezoglou and Krasakopoulou, 2002) within the LIW water masses that are nutrient-enriched commonly due to the degradation of the sinking organic matter carried by the BSW (Frangoulis et al., 2010; Souvermezoglou et al., 2014). Apparently, currents and circulation patterns of the North Aegean have an impact on the distribution of coccolithophore assemblages and convert them while sinking from the euphotic zone to the seafloor. For the comparison of the living plankton community with the sinking assemblage, an assemblage without *F. profunda* has been considered for the sediment trap time series (Fig. 4c). In this case, the *E. huxleyi* mean annual (up to ~85%) and mean relative abundance (~95%) during January and April fit relatively well with the plankton mean (Fig. 4a, c).

Obviously, the absence of *F. profunda* in the plankton samples is a result of the sampling depth limitation; however, a number of other taxa are recognised to have been lost while sinking to the seabed (Appendix 1), probably due to biostratonomical (post-mortem) processes. Syracosphaeraceae presented a rich variety of species

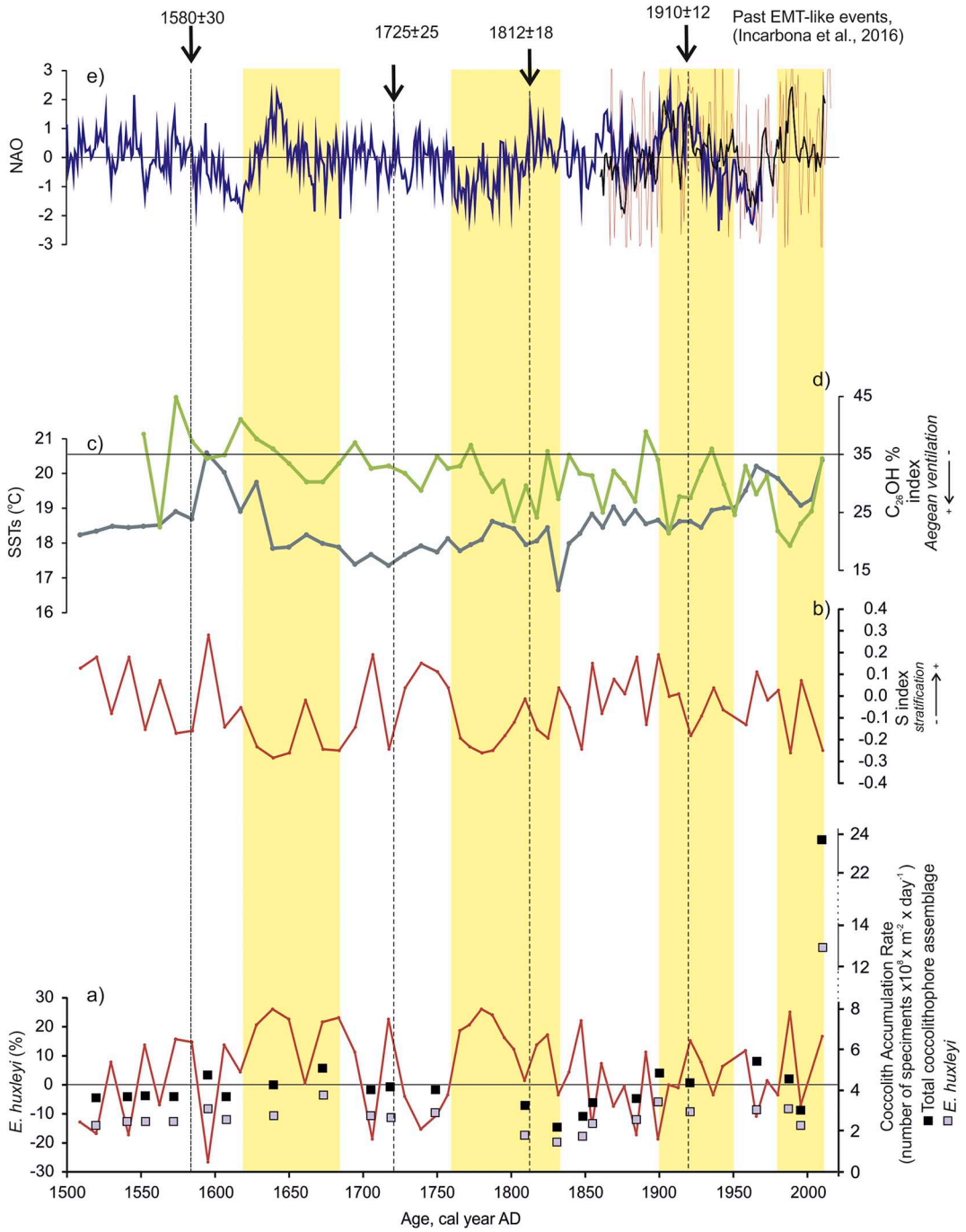

Fig. 6. a. *Emiliania huxleyi* mean (M2 multicore sediment record) in terms of anomalies with respect to the 1855–1955 mean and coccolith accumulation rates (total calcareous nannofossils and *E. huxleyi*), b. Stratification S-index as the ratio between *F. profunda* (F) and *E. huxleyi* (E) abundances S = F/F + E (from Gogou et al., 2016), c. reconstructed alkenone SSTs (°C) for the M2 sediment record (from Gogou et al., 2016), d. Ventilation C26OH%index as the relative proportion of n-hexacosan-1-ol (C_{26}OH) to the sum of C_{26}OH plus n-nonacosane (C_{29}) (from Incarbona et al., 2016), e. NAO-index [compiled from datasets of Ortega et al. (2015) (cyan), Hurrell et al., 2017 (purple) and Hurrell et al., 2017 5-year running means (black)].
Shaded yellow bands represent "*E. huxleyi* dominance" intervals at 1980–present, 1900–1950, 1760–1840 and 1620–1680 years AD. (For interpretation of the references to colour in this figure legend, the reader is referred to the web version of this article.)

composition in the living community including *S. ampliora, S. anthos, S. corolla, S. histrica, S. mediterranea, S. molischii, S. nodosa, S. ossa, S. prolongata, S. protrudens, S. pulchra, S. tumularis, C. rigidus, O. formosus.* Interestingly, Syracosphaeraceae diversity in the export fluxes was limited to *S. pulchra* and *S. mediterranea*. Compared to plankton samples the holococcolithophore group in the sediment traps was restricted only to *Syracolithus dalmaticus*, *S. mediterranea* HOL *wettsteinii* type and *Helicosphaera carteri* HOL perforate type. Overall, most of the fragile holococcolithophore species and the delicate *A. robusta, Acanthoica quattrospina, Cyrtosphaera lecaliae, Helicosphaera pavimentum* and *Alisphaera unicornis* were constrained in the Aegean water column (Figs. 3–4), while their coccoliths were missing in the sinking record and surface sediment due to either dissolution or, more likely, due to destruction during grazing.

Cachão and Oliveira (2000) consider the coccolith/coccosphere ratio as a useful ecological index, which, however, needs to be adjusted

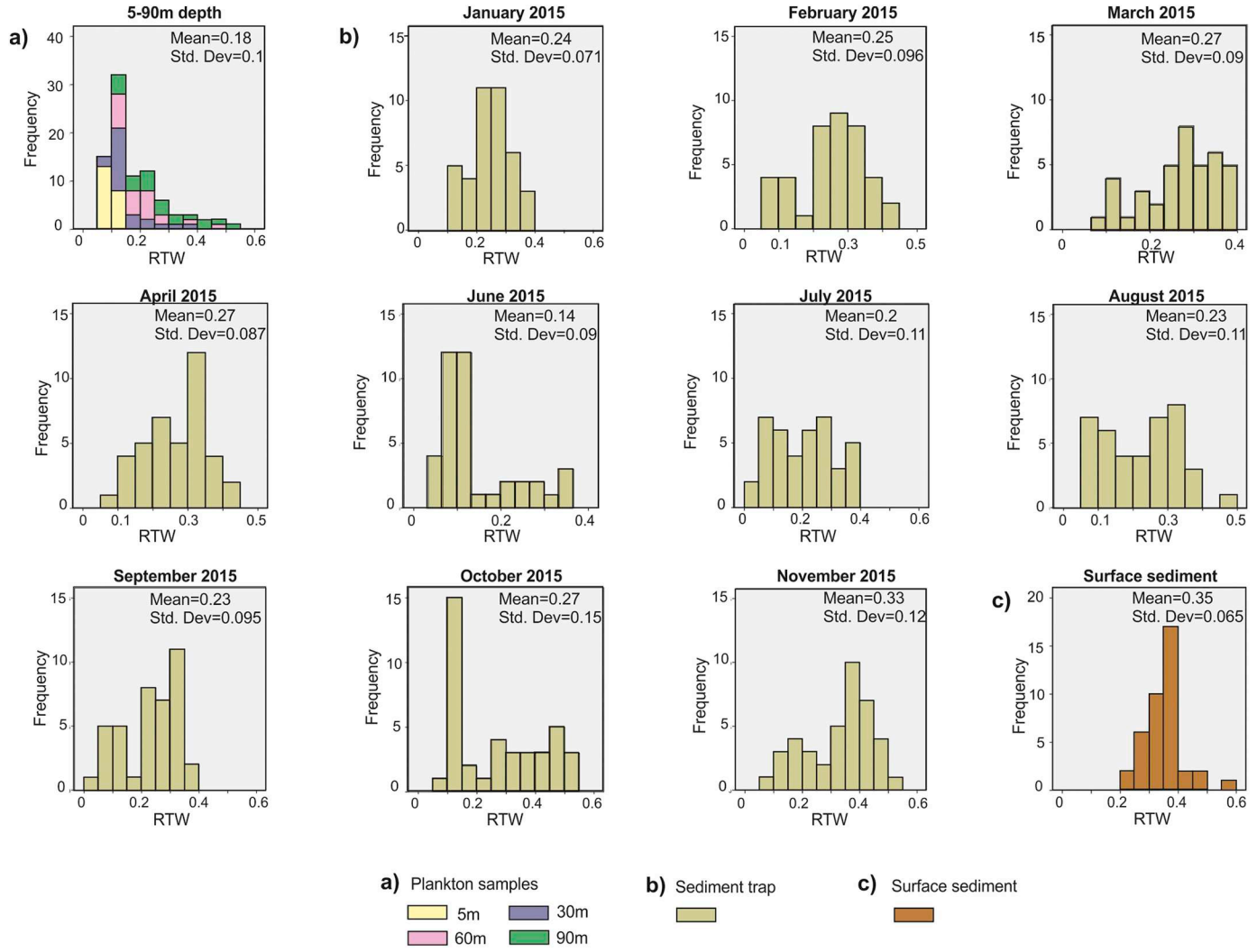

Fig. 7. Relative tube width (RTW) histograms of the species *E. huxleyi* at site M2, a) plankton samples, b) sediment trap series, c) surface sediment. For details see Appendix 2.

to the various species ecological preferences. In the present study, the "coccolith excess" (see above) has been calculated to observe potential seasonal variations in the predominance of vertical export processes and lateral/vertical transport (Fig. 4d). The noticeable small peaks in the "coccolith excess" during certain warm months, e.g., in June 2011 (Fig. 4d), are considered to reflect the surface productivity (Fig. 4d) that shows moderate Chl-a values (Fig. 2a). Interestingly, the extreme minima of the "coccolith excess" in late February 2015 indicates the strong dominance of vertical export, in agreement to the strong high productivity peak of the same month as also suggested by the total coccosphere flux (Fig. 4d). Chl-a maxima in late winter - early spring 2015 (Fig. 2a) strongly support the enhanced productivity. Nevertheless, an extreme flux peak might be representative of higher production, less dissolution, less dilution and/or faster settling (Koebrich et al., 2016). Such a 'pulse-like sedimentation event' (Nowald et al., 2006) may reflect a fast settling following an episode of enhanced productivity (e.g., Koebrich et al., 2016). The increased precipitation during the considered time interval (Fig. 2a) has most probably triggered increased river runoffs in the North Aegean (Fig. 2b), drastically affecting the lithogenic flux; data from the North Aegean sediment trap further support this hypothesis since the contemporaneous lithogenic flux peaks propose a reinforcing factor for fast particle sinking. In particular, higher peaks in the lithogenic flux in-between January and March 2015 compete with the extreme minima of the "coccolith excess" (Fig. 4d), suggesting that the observed "excess" pattern is associated with greater vertical export due to high productivity peak followed by rapid settling and/or enhanced grazing.

5.2. Coccolithophore response to the regional hydrographic regime

Sediment trap coccolith data in addition to coccosphere counts can provide a better description of the ecological and biostratonomical (post-mortem) status of the coccolithophore species (e.g., Cachão and Oliveira, 2000; Ziveri et al., 1999; Triantaphyllou et al., 2004). The North Aegean "coccolith excess" parameter that is linked to high productivity season (Fig. 4d), actually reveals the "low sphere-lith correlation" model of Cachão and Oliveira (2000), implying a relatively recent development of the cells with a few detached liths. Yet, the *E. huxleyi* dominance in the area during the whole annual cycle and the remarkable seasonal peak this species displays (e.g., late winter - spring) denote the question of the species in-situ productivity vs. additional *E. huxleyi*-enriched water mass influx. Also, the coccolithophore assemblage composition as well as the detailed morphometric analyses of the *E. huxleyi* coccolith calcification degree can contribute in tracing the origin of species various morphotypes that are directly linked to the various water masses in the North Aegean water column.

Traditionally, the BSW inflows play a critical role in the North Aegean oceanography, forming a surface fresher water lid (Fig. 1) and

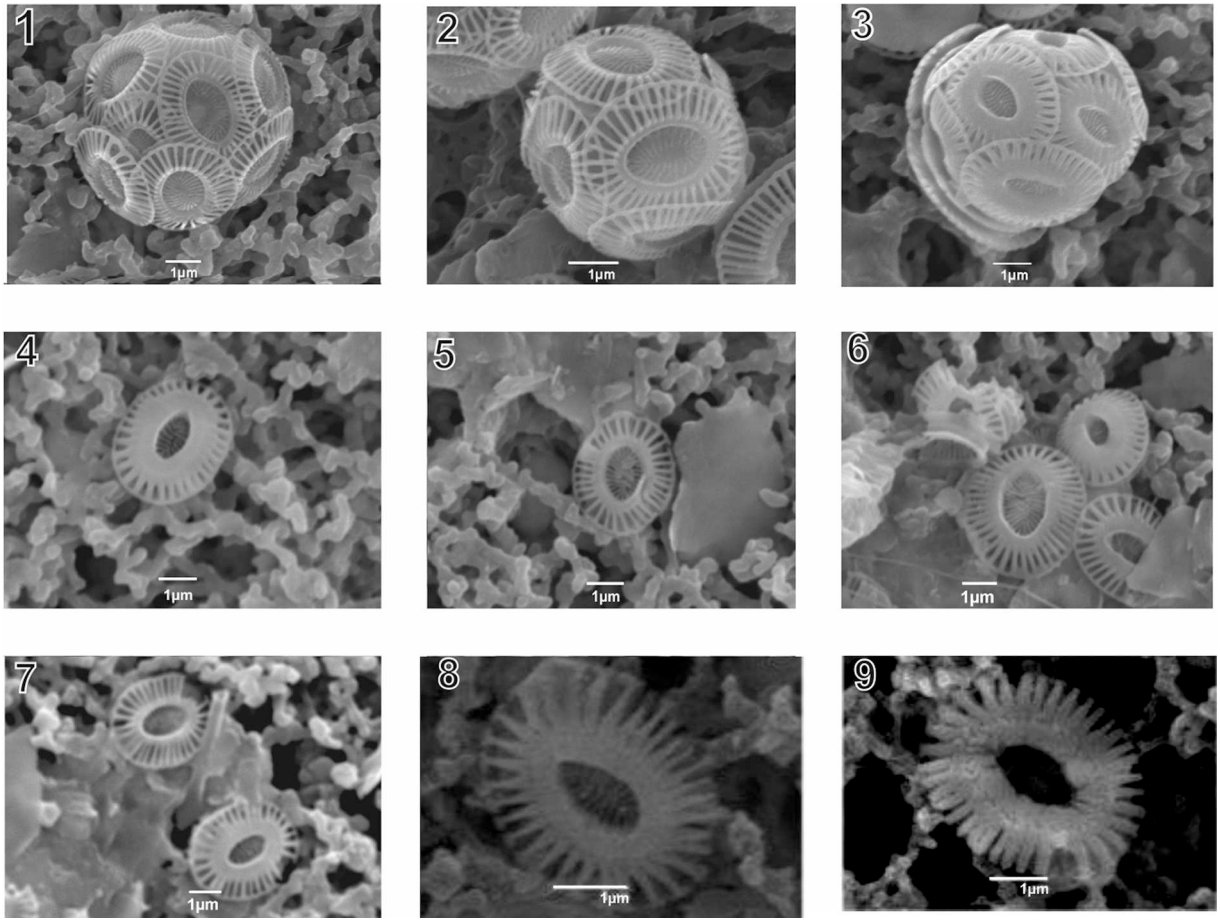

Plate 1. 1, **2**: *Emiliania huxleyi* lightly calcified morphotypes from plankton samples (May 2011; 5 m, 30 m depth), tracing BSW inflow. **3**: *E. huxleyi* heavier calcified morphotypes from plankton samples (May 2011; 60 m, 90 m depth), tracing LW masses. **4–7**: *E. huxleyi* coccoliths from sediment trap samples in February (**4**, **5**, **6**) and October 2015 (**7**), featured by bimodal distribution of RTW with both lightly and seasonally controlled heavily calcified morphotypes associated with the concurrent presence of enhanced surface BSW inflows and deeper LW masses. **8–9**: Surface sediment revealed *E. huxleyi* RTW unimodal distribution dominated by highly calcified specimens.

resulting in stratification control of the North Aegean water column (Zervakis et al., 2000, 2004; Velaoras and Lascaratos, 2010; Velaoras et al., 2013). Surficial BSW masses carry impressive, almost monospecific coccolithophore assemblages composed of lightly calcified *E. huxleyi* morphotypes (Triantaphyllou et al., 2014; Ravani et al., 2017). These morphotypes have been documented to prevail in BSW all year round (RTW at ~0.10; Karatsolis et al., 2017), whereas, in contrast, the Levantine water (LW) masses in North Aegean are featured by more heavily calcified coccoliths during the low SST winter-spring season (Triantaphyllou et al., 2010), which is typical for the SE Mediterranean (D'Amario et al., 2018). In addition, D'Amario et al. (2018) further supported the correlation between *E. huxleyi* type A calcification varieties and oceanographic parameters such as water carbonate chemistry, salinity, nutrients and temperature. Therefore, the performed morphometric analysis on the *E. huxleyi* coccoliths within the context of the present study provided insight into their origin as well as the coccolithophore transfer route through the different North Aegean water masses. Indeed, plankton samples from May 2011 (see Plate 1) revealed the notable presence of lightly calcified *E. huxleyi* coccoliths in the upper water column layers (RTW at 0.05–0.10; Fig. 7a), associated with the elevated less saline (34–36) BSW intrusion during the increased SST (~17.27° C) period (e.g., Zervakis et al., 2000; Lagaria et al., 2017). The inverse trend of SST with the RTW values (Figs. 2a, 7a) is supported by the statistical correlation presented in Table 2. Moreover, the positive correlation between Chl-a and increased calcification can be verified by the unimodal distribution appearing in late winter - early spring 2015 (Figs. 2a, 7a; Table 2). Interestingly, the outstanding negative shift in the "coccolith excess" pattern (Fig. 4d) linked to the exceptional *E. huxleyi* relative abundance in late February 2015 is reflected by a distinct RTW bimodal distribution (values between 0.05 and 0.40; Fig. 7b). As the sediment trap captures the signal of more than one water mass, the increase in lightly calcified morphotypes (high frequency of values of ~0.10) can be considered as the straightforward effect of enhanced BSW inflow in addition to the heavier calcified *E. huxleyi* coccoliths coming from LW masses flowing under the BSW lid. This explains the absence of a seasonal unimodal calcification pattern so far recorded in the Aegean (Triantaphyllou et al., 2010; D'Amario et al., 2018), implying the occurrence of at least two morphotypes during the same season with the question whether this is a genotypic or ecophenotypic causal effect remaining unanswered. Likewise, the increase in low calcified coccoliths during October–November 2015 (Plate 1, Fig. 7b) evidences once more the surficial BSW intrusion to the Athos Basin, also described in October 2013 by Karatsolis et al. (2017). Hitherto, the seasonally-controlled presence of lightly calcified specimens from the deeper LW layers cannot be excluded (Plate 1, Fig. 7b). In contrast, the RTW bimodal mode in August–September 2015 more likely indicates both light and heavier calcified LW-origin morphotypes, as the blowing northerly winds deflect the BSW from Athos Basin to the southeastern parts of the North Aegean.

5.3. Evaluating calcareous nannofossil paleoenvironmental proxies in the North Aegean fossil record

The surface sediment and the sedimentary record for the last 500 years have been used to achieve a better knowledge regarding the linkage of the North Aegean extant coccolithophore communities to the fossil assemblages and their response to the prevalent environmental regimes. Interestingly, the multiannual mean fluxes (2011–2015: 20×10^8 coccoliths $m^2\,day^{-1}$; Fig. 4b) demonstrated similar values to the accumulation rates recorded in the surface sediment (23.6×10^8 coccoliths $m^{-2}\,day^{-1}$; Fig. 5a). This remarkable similarity implies that the coccolith AR in the sediment record may represent a valuable proxy for the reconstruction of past water column fluxes. Coccoliths mostly sink in the zooplankton faecal pellets or as macro-aggregates, so that their sinking speed is relatively high and potentially triggered by phytoplankton blooms (Nowald et al., 2006). The sinking speed of such densely-packed pellets has been observed to reach up to 570 m d^{-1} (Fischer and Karakas, 2009), so even though several studies have recorded a decrease in the diversity of species and preservation of more heavily calcified taxa, the main features of the living assemblages are commonly maintained in the surface sediments (Baumann et al., 2000; Koebrich et al., 2016; Saavedra-Pellitero and Baumann, 2015). The present results indicate that *E. huxleyi* dominated in both North Aegean export flux (mean AR of 14.07×10^8 coccoliths $m^2\,day^{-1}$) and surface sediment assemblages with estimated values of 12.87×10^8 coccoliths $m^2\,day^{-1}$. In contrast, *F. profunda* represented a minor component of the export flux assemblage (mean 2011–2015: 2.27×10^8 coccoliths $m^2\,day^{-1}$) compared to the 2000–2010, time span that is reflected in the surface sediment (7.42 87 $\times 10^8$ coccoliths $m^2\,day^{-1}$). However, this should be reasonably expected when concerning the dissimilarity of the compared time intervals as well as the impact of circulation patterns and accumulation processes on the route of the species tiny coccoliths towards the bottom sediment.

Calcareous nannofossils in the surface sediment (0–1 cm) most likely represent the extant assemblage composition of the cold season (December–April, Fig. 3b), with *E. huxleyi* (~60%) prevailing over *F. profunda* (32%) (Fig. 5a), reflecting the annual cycle highest productivity period (e.g., Barcena et al., 2004). Despite that both BSW and LW masses-origin *E. huxleyi* coccolith morphotypes were sinking to the seabed, the surface sediment at the North Aegean M2 site revealed a unimodal distribution dominated by highly calcified specimens (RTW values >0.20; Fig. 7c, Plate 1). This could be attributed to processes of secondary calcite overgrowth (e.g., Raffi and De Bernardi, 2008) and/or prevention of lightly calcified *E. huxleyi* coccoliths to accumulate on the seafloor either because they are drifted by the overlying isolated BSW flow towards its southwestern pathway (e.g., Androulidakis et al., 2012) or due to their low contribution to the total *E. huxleyi* in-situ productivity. Apparently the in-situ productivity in winter - early spring resulting in *E. huxleyi* relative abundance maxima, which follow the Chl-a maxima and SST minima (Fig. 2a), favors the accumulation of the highly calcified morphotype coccoliths on the seafloor. Thus, additional factors other than single *E. huxleyi* morphology are apparently needed to evaluate the BSW influx within the sediment record (e.g., Herrle et al., 2018), taking into account that the accumulation of lightly calcified morphotypes along the sediment record may also reflect the species seasonal calcification pattern in the LW masses.

The prominent domination of *E. huxleyi* over *F. profunda* especially indicated by the 2014–15 time series data (Fig. 3b) reveals an almost non-stratified water column with ventilation events (e.g., Dimiza et al., 2015; Gogou et al., 2016; Triantaphyllou et al., 2014). These conditions correspond to an on-going process verified as responsible for the periodical activation of the Aegean as a dense water formation source area. Deep-water formation in the North Aegean has been reported as the EMT event during the late 1980s to early-mid 1990s (Theocharis et al., 1999), whereas remarkable recent production of dense waters since 2003, but with various fluctuations (Krokos et al., 2014; Theocharis et al., 2014), is associated with strong heat loss comparable to the EMT peak period. Similar EMT-like events have been described in the recent fossil record (last 500 years; Gogou et al., 2016; Incarbona et al., 2016), with positive shifts of the North Atlantic Oscillation (NOA) coupled with Aegean waters' significant cooling, increased salinity in the Levantine Basin and surface water freshening in the Sicily Channel. The modern Aegean coccolithophore accumulation is practically *E. huxleyi*-based, with species relative abundance reaching ~60% (Fig. 4b), indicating enhanced water column mixing (e.g., Dimiza et al., 2015; this study) being well associated with a positive NAO trend, especially when regarding the 2014–15 time interval (Fig. 4b). Although plankton and sediment trap data are not available for the prominent NAO negative peaks (e.g., 2010), the last observation may be considered as an added value when using calcareous nannofossil assemblage fluctuations as high-resolution paleoenvironmental proxies of the North Aegean paleoceanographic variability during the recent past.

Despite that fossil assemblages might get influenced by dissolution effects and sedimentological processes (e.g., Andruleit et al., 2004; Barcena et al., 2004; Baumann et al., 2005; Dimiza and Triantaphyllou, 2010), the studied North Aegean sedimentary record of the last 500 years is featured by periodic change in the dominance of *E. huxleyi* (~30–80%, mean ~60%) over *F. profunda* and other minor species (Fig. 5c), with conspicuous peaks during the 1980–present, 1900–1950, 1760–1840 and 1620–1680 time spans (Fig. 5c). During these "*E. huxleyi* dominance" intervals, the calcareous nannofossil pattern suggests a non-stratified water column (low S-index) and relatively low SST values (Fig. 6b, c). These conditions are compatible with the modern cold season (November–April) coccolithophore productivity and calcareous nannoplankton export flux, notably expressed by the 2014–15 time series data (Fig. 3b). Interestingly, calcareous nannofossil data present an opposite trend to the C_{26}OH% (Fig. 6d; Incarbona et al., 2016), an organic chemical index reflecting oxygenation variability (Martrat et al., 2007), with *E. huxleyi* bulge peaks (~60%) corresponding, in general, to positive NAO shifts. Hence, the prominent *E. huxleyi* peak in the sediment record during 1988 (Fig. 5c) is remarkably linked to the EMT event of 1988–1995. These conditions were related to increased Aegean evaporation and enhanced cyclonic activity over the Eastern Mediterranean that triggered exceptionally cold air over the Aegean (Romanski et al., 2012), favouring surface buoyancy loss and deep-water formation in the North Aegean Basin. Incarbona et al. (2016) have identified a series of EMT-like events in 1910 ± 12, 1812 ± 18, 1725 ± 25 and 1580 ± 30 coupled either with positive NAO shifts and/or reduced solar activity and strong volcanic eruptions. An exception stands for the interval 1760–1840 (Fig. 6a, e), in which the *E. huxleyi* increments and the concomitant drop of the stratification S-index (Fig. 6a, b) seem to be associated with the cold shift of 1832 ± 15 (Fig. 6c; Gogou et al., 2016), related to global near-surface cooling driven by volcanic forcing (e.g., Tambora volcanic eruption; Stothers, 1984) within the Dalton solar minimum (1790–1830; e.g., Wagner and Zorita, 2005).

The present study appraises that the *E. huxleyi* relative abundance of ~60% can be considered as a useful index for evaluating past EMT-like events. All major intermediate-to-deep overturning perturbations already recorded in the Aegean Sea are recognised within the "*E. huxleyi* dominance" intervals (Fig. 6), while an additional event may be proposed for the 1620–1680 time interval, providing strong evidence for Aegean ventilation during a prominent positive NAO phase around 1640 (Fig. 6).

Finally, the high calcareous nannoplankton ARs observed within the positive NAO peaks of the last 500 years (Fig. 6e), suggest either higher coccolithophore productivity during these intervals or enhanced sinking parameters such as particles forming aggregates. The "*E. huxleyi* dominance" intervals prove to last longer than the "*F. profunda* dominance" counterparts, while, similarly to the surface sediment composition, minor species abundance appears enhanced during the "*E. huxleyi* dominance" intervals (Fig. 4a). High *F. profunda* abundances (e.g.,

in 1899, 1884, 1854, 1757–1706, 1595, 1541, 1509–1520), linked to high S-index and SST values (Fig. 6b, c), indicate stratified water column conditions associated with a deeper nutricline (e.g., Molfino and McIntyre, 1990) and potentially enhanced BSW influx (e.g., Karatsolis et al., 2017).

6. Conclusions

The analysis of plankton and sediment trap samples (2011–2015) from the sampling site M2 in the Athos Basin of the North Aegean Sea and their comparison with data obtained from the surface sediment of the same location provides valuable information about the modifications evolving in most common coccolithophores during their export from the euphotic zone and their sinking to the sea bottom. The main conclusions are summarised as follows:

- *Emiliania huxleyi* dominated in the plankton, sediment trap and surface sediment calcareous nannoplankton assemblages, occasionally reaching extreme abundances in the present-day North Aegean waters. Notably, *Florisphaera profunda* was not included in the plankton assemblage, but this was most probably due to sampling depth limitations. Plankton samples revealed a well-developed upper euphotic zone community but several fragile *Syracosphaera* and holococcolithophore species were probably lost while sinking to the seabed.

- Sediment trap calcareous nannoplankton fluxes presented similar values to the accumulation rates recorded in the surface sediment dating back to 2000–2010. Apart from the loss of the more fragile holococcolithophore species and the delicate *Algirosphaera robusta,* the main features of the living assemblages were generally preserved on the seafloor.

- Morphometric analysis of the *E. huxleyi* regarding the degree of coccolith calcification, contributed to the investigation of the water masses in the North Aegean water column. The presence of lightly calcified morphotypes in the plankton and sediment trap samples indicated enhanced surficial Black Sea water inflows during May 2011, February 2015 and October 2015 in addition to the heavier calcified *E. huxleyi* coccoliths originating from Levantine water masses flowing deeper. This explains the absence of a seasonal unimodal calcification pattern so far recorded in the Aegean Sea, implying the presence of at least two *E. huxleyi* morphotypes during the same season. However, this signal was not preserved in the surface sediment assemblage due to processes of secondary calcite overgrowth and/or water circulation patterns impact preventing the accumulation of the lightly calcified *E. huxleyi* on the seafloor.

- The coccolithophore assemblage of the past 500 years revealed a periodic occurrence of "*E. huxleyi* dominance" intervals (~60%), indicating strong water column convection coupled with NAO positive shifts and volcanic activity within the Dalton solar minimum. In contrast, the analogous occurrence of "*F. profunda* dominance" intervals may be linked to high S-index and SST values, revealing stratified conditions in the water column, potentially associated with increased BSW intrusion.

Acknowledgements

The funding for the fulfilment of this study was provided by the Greek National Project KRIPIS (Integrated Observatories in the Greek Seas - IO, HCMR-MIS 451724; NSRF), the European Research Project MedEcos (MarinERA, EU/FP6) and the IKYDA program of the DAAD (project 57260124 AegeanCocco). The first author E. Skampa has been granted with a scholarship from the State Scholarships Foundation. This research is co-financed by Greece and the European Union (European Social Fund- ESF) through the Operational Programme "Human Resources Development, Education and Lifelong Learning" in the context of the project "Strengthening Human Resources Reaserch Potential via Doctorate Research" (MIS-5000432), implemented by the State Scholarships Foundation (IKY). Also, we would like to thank the two anonymous reviewers and the journal chief editor Dr. Richard Jordan for their constructive comments that significantly helped us to improve the quality of this manuscript during the revision process.

Appendix A. Supplementary data

Supplementary data to this article can be found online at https://doi.org/10.1016/j.marmicro.2019.03.001.

References

Acker, J.G., Leptoukh, G., 2007. Online Analysis Enhances Use of NASA Earth Science Data. Eos Trans. AGU 88 (2), 14–17.
Androulidakis, Y.S., Kourafalou, V.H., Krestenitis, Y.N., Zervakis, V., 2012. Variability of deep water mass characteristics in the North Aegean Sea: the role of lateral inputs and atmospheric conditions. Deep-Sea Res.Part I Oceanogr. Res. Pap. 67, 55–72.
Andruleit, H., 1997. Coccolithophore fluxes in the Norwegian-Greenland Sea: seasonality and assemblage alterations. Mar. Micropaleontol. 31, 45–64.
Andruleit, H., Rogalla, U., Stager, S., 2004. From living communities to fossil assemblages: origin and fate of coccolithophores in the northern Arabian Sea. In: Triantaphyllou, M. (Ed.), Advances in the Biology, Ecology and Taxonomy of Extant Calcareous Nannoplankton. Micropaleontology, vol. 50. pp. 5–21.
Athanasiou, M., Bouloubasi, I., Gogou, A., Klein, V., Dimiza, M.D., Parinos, C., Skampa, E., Triantaphyllou, M.V., 2017. Sea surface temperatures and environmental conditions during the "warm Pliocene" interval (~4.1–3.2 Ma) in the Eastern Mediterranean (Cyprus). Glob. Planet. Chang. 150, 46–57.
Bairbakhish, A.N., Bollmann, J., Sprengel, C., Thierstein, H.R., 1999. Disintegration of aggregates and coccospheres in sediment trap samples. Mar. Micropaleontol. 37, 219–223.
Barcena, M.A., Flores, J.A., Sierro, F.J., Perez-Folgado, M., Fabres, J., Calafat, A., Canals, M., 2004. Planktonic response to main oceanographic changes in the Alboran Sea (Western Mediterranean) as documented in sediment traps and surface sediments. Mar. Micropaleontol. 53, 423–445.
Baumann, K.-H., Andruleit, H.A., Samtleben, C., 2000. Coccolithophores in the Nordic Seas: comparison of living communities with surface sediment assemblages. Deep-Sea Res. II 47, 1743–1772.
Baumann, K.-H., Andruleit, H., Bockel, B., Geisen, M., Kinkel, H., 2005. The significance of extant coccolithophores as indicators of ocean water masses, surface water temperature, and paleoproductivity: a review. Paläontol. Z. 79 (1), 93–112.
Beaufort, L., Probert, I., de Garidel-Thoron, T., Bendif, E.M., Ruiz- Pino, D., Metzl, N., Goyet, C., Buchet, N., Coupel, P., Grelaud, M., Rost, B., Rickaby, R.E.M., de Vargas, C., 2011. Sensitivity of coccolithophores to carbonate chemistry and ocean acidification. Nature 476, 80–83.
Boeckel, B., Baumann, K.-H., 2008. Vertical and lateral variations in coccolithophore community structure across the subtropical frontal zone in the South Atlantic Ocean. Mar. Micropaleontol. 67, 255–273.
Bolton, C.T., Hernandez-Sanchez, M.T., Fuertes, M.A., Gonzalez-Lemos, S., Abrevaya, L., Mendez-Vicente, A., Flores, J.-A., Probert, I., Giosan, L., Johnson, J., Stoll, H.M., 2016. Decrease in coccolithophore calcification and CO_2 since the middle Miocene. Nat. Commun. 7, 10284. (2016). https://doi.org/10.1038/ncomms10284.
Bonomo, S., Grelaud, M., Incarbona, A., Malinverno, E., Placenti, F., Bonanno, A., Di Stefano, E., Patti, B., Sprovieri, M., Genovese, S., Rumolo, P., Mazzola, S., Zgozi, S., Ziveri, P., 2012. Living coccolithophores from the Gulf of Sirte (Southern Mediterranean Sea) during the summer of 2008. Micropaleontology 58, 487–503.
Bonomo, S., Cascella, A., Alberico, I., Lirer, F., Vallefuoco, M., Marsella, E., Ferraro, L., 2018. Living and thanatocoenosis coccolithophore communities in a neritic area of

the Central Tyrrhenian Sea. Mar. Micropaleontol. 142, 67–91.
Cachão, M., Oliveira, A., 2000. (Cocco)liths versus (cocco)spheres: approaching the ecological performance of coccolithophores. J. Nannoplankton Res. 22, 29–34.
D'Amario, B., Ziveri, P., Grelaud, M., Oviedo, A., 2018. *Emiliania huxleyi* coccolith calcite mass modulation by morphological changes and ecology in the Mediterranean Sea. PLoS One 13 (7), e0201161. https://doi.org/10.1371/journal.pone.0201161.
Dimiza, M.D., Triantaphyllou, M.V., 2010. Comparing living and Holocene coccolithophore assemblages in the Aegean marine environments. Bull. Geol. Soc. Greece 2010.
Dimiza, M., Triantaphyllou, M.V., Dermitzakis, M.D., 2008. Seasonality and ecology of living coccolithophores in E. Mediterranean coastal environments (Andros Island, Middle Aegean Sea). Micropaleontology 54, 159–175.
Dimiza, M., Triantaphyllou, M.V., Malinverno, E., Psarra, S., Karatsolis, B.T., Mara, P., Lagaria, A., Gogou, A., 2015. The composition and distribution of living coccolithophores in the Aegean Sea (NE Mediterranean). Micropaleontology 61, 521–540.
Fischer, G., Karakas, G., 2009. Sinking rates of particles in biogenic silica- and carbonate-dominated production systems of the Atlantic Ocean: implications for the organic carbon fluxes to the deep ocean. Biogeosciences 6, 85–102.
Frangoulis, C., Psarra, S., Zervakis, V., Meador, T., Mara, P., Gogou, A., Zervoudaki, S., Giannakourou, A., Pitta, P., Lagaria, A., Krasakopoulou, E., Siokou-Frangou, I., 2010. Connecting export fluxes to plankton food-web efficiency in the Black Sea waters inflowing into the Mediterranean Sea. J. Plankton Res. 32, 1203–1216.
Gogou, A., Triantaphyllou, M., Xoplaki, E., Izdebski, A., Parinos, C., Dimiza, M., Bouloubassi, I., Luterbacher, J., Kouli, K., Martrat, B., Toreti, A., Fleitmann, D., Rousakis, G., Kaberi, H., Athanasiou, M., Lykousis, V., 2016. Climate variability and socio-environmental changes in the northern Aegean (NE Mediterranean) during the last 1500 years. Quat. Sci. Rev. 136, 209–228.
Herrle, J.O., Bollmann, J., Gebuhr, C., Sculz, H., Sheward, R.M., Giesenberg, A., 2018. Black Sea outflow response to Holocene meltwater events. Sci. Rep. 8, 4081.
Hurrell, James, National Center for Atmospheric Research Staff (Eds.), 2017. The Climate Data Guide: Hurrell North Atlantic Oscillation (NAO) Index (station-based), Last modified 07 Nov 2017. Retrieved from. https://climatedataguide.ucar.edu/climate-data/hurrell-north-atlantic-oscillation-nao-index-station-based.
Ignatiades, L., Psarra, S., Zervakis, V., Pagou, K., Souvermezoglou, E., Assimakopoulou, G., Gotsis-Skretas, O., 2002. Phytoplankton size-based dynamics in the Aegean Sea (Eastern Mediterranean). J. Mar. Syst. 36, 11–28.
Ignatiades, L., Gotsis-Skretas, O., Pagou, K., Krasakopoulou, E., 2009. Diversification of phytoplankton community structure and related parameters along a large-scale longitudinal east–west transect of the Mediterranean Sea. J. Plankton Res. 31, 411–428.
Incarbona, A., Matrat, B., Mortyn, G.P., Sprovieri, M., Ziveri, P., Gogou, A., Jorda, G., Xoplaki, E., Luterbacher, J., Langone, L., Marino, G., Rodriguez-Sanz, L., Triantaphyllou, M., Di Stefano, E., Grimalt, J.O., Tranchida, G., Spriovieri, R., Mazzola, S., 2016. Mediterranean circulation perturbations over the last five centuries: Relevance to past Eastern Mediterranean Transient-type events. Sci. Rep. 6, 29623.
Karageorgis, A.P., Kontoyiannis, H., Stavrakakis, S., Krasakopoulou, E., Gogou, A., Papadopoulos, A., Kanellopoulos, Th.D., Rousakis, G., Malinverno, E.., Triantaphyllou, M.V., Lykousis, V., 2018. Particle dynamics and fluxes in canyons and open slopes of the southern Cretan margin (Eastern Mediterranean). Prog. Oceanogr. https://doi.org/10.1016/j.pocean.2017.12.009.
Karatsolis, B.-Th., Triantaphyllou, M.V., Dimiza, M.D., Malinverno, E., Lagaria, A., Mara, P., Archontikis, O., Psarra, S., 2017. Coccolithophore assemblage response to Black Sea Water inflow into the North Aegean Sea (NE Mediterranean). Cont. Shelf Res. 149, 138–150.
Kleijne, A., 1991. Holococcolithophorids from the Indian Ocean, Red Sea, Mediterranean Sea and North Atlantic Ocean. Mar. Micropaleontol. 17, 1–76.
Koebrich, M.I., Baumann, K.-H., Fischer, G., 2016. Seasonal and inter-annual dynamics of coccolithophore fluxes from the upwelling region off Cape Blanc, NW Africa. J. Micropaleontol. 35, 103–116.
Krokos, G., Velaoras, D., Korres, G., Perivoliotis, L., Theocharis, A., 2014. On the continuous functioning of an internal mechanism that drives the Eastern Mediterranean thermohaline circulation: the recent activation of the Aegean Sea as a dense water source area. J. Mar. Syst. 129, 484–489.
Lagaria, A., Mandalakis, M., Mara, P., Frangoulis, C., Karatsolis, B.-Th., Pitta, P., Triantaphyllou, M., Tsiola, A., Psarra, S., 2017. Phytoplankton variability and community structure in relation to hydrographic features in the NE Aegean frontal area (NE Mediterranean Sea). Cont. Shelf Res. 149, 124–137. https://doi.org/10.1016/j.csr.2016.07.014.
Lagaria, A., Psarra, S., Gogou, A., Tuğrul, S., Christaki, U., 2013. Particulate and dissolved primary production along a pronounced hydrographic and trophic gradient (Turkish Straits System-NE Aegean Sea). J. Mar. Syst. 119–120, 1–10.
Lascaratos, A., 1992. Hydrology of the Aegean Sea. In: Charnock, H. (Ed.), Winds and currents of the Mediterranean basin. Harvard University, Cambridge, MA, pp. 313–334 NATO Advanced Science Institute: Atmospheric and Oceanic Circulation in the Mediterranean basin, no. 40.
Lykousis, V., Chronis, G., Tselepides, A., Price, N.B., Theocharis, A., Siokou-Fragou, I., Van Wambeke, F., Danovaro, R., Stavrakakis, S., Duineveld, G., Georgopoulos, D., Ignatiades, L., Souvermezoglou, A., Voutsinou-Taliadouri, F., 2002. Major outputs of the recent multidisciplinary biogeochemical researches undertaken in the Aegean Sea. J. Mar. Syst. 33–34, 313–334.
Malinverno, E., Ziveri, P., Corselli, C., 2003. Coccolithophorid distribution in the Ionian Sea and its relationship to eastern Mediterranean circulation during late fall-early winter 1997. J. Geophys. Res. 108 (9), 8115. https://doi.org/10.1029/2002JC001346.
Malinverno, E., Triantaphyllou, M.V., Stavrakakis, S., Ziveri, P., Lykousis, V., 2009. Seasonal and spatial variability of coccolithophore export production at the South-Western margin of Crete (Eastern Mediterranean). Mar. Micropaleontol. 7, 131–147.
Malinverno, E., Maffioli, P., Corselli, C., De Lange, G., 2014. Present-day fluxes of coccolithophores and diatoms in the pelagic Ionian Sea. J. Mar. Syst. 132, 13–27.
Malinverno, E., Karatsolis, B.-Th, Dimiza, M.D., Triantaphyllou, M.V., 2016. Extant silicoflagellates from the Northeast Aegean (eastern Mediterranean Sea): morphologies and double skeletons. Rev. Micropaleontol. 59, 253–265.
Martrat, B., Grimalt, J.O., Shackleton, N.J., de Abreu, L., Hutterli, M.A., Stocker, T.F., 2007. Four climate Cycles of Recurring deep and Surface Water Destabilizations on the Iberian margin. Science 317, 502–507.
Molfino, B., McIntyre, A., 1990. Precessional forcing of nutricline dynamics in the equatorial Atlantic. Science 249, 766–769.
Negri, A., Giunta, S., 2001. Calcareous nannofossil paleoecology in the sapropel S1 of the Eastern Ionian Sea: paleoceanographic implications. Palaeogeogr. Palaeoclimatol. Palaeoecol. 169, 101–112.
Nowald, N., Karakas, G., Ratmeyer, V., Fischer, G., Schlitzer, R., Davenport, R.A., Wefer, G., 2006. Distribution and transport processes of marine particulate matter off Cape Blanc (NW-Africa): results from vertical camera profiles. Ocean Sci. Discuss. 3, 903–938.
Parker, D.E., Folland, C.K., Jackson, M., 1995. Marine surface temperature: observed variations and data requirements. Clim. Chang. 31, 559–600.
Poulos, S.E., Drakopoulos, P.G., Collins, M.B., 1997. Seasonal variability in sea surface oceanographic conditions in the Aegean Sea (Eastern Mediterranean): an overview. J. Mar. Syst. 13, 225–244.
Raffi, I., De Bernardi, B., 2008. Response of calcareous nannofossils to the Paleocene–Eocene thermal Maximum: Observations on composition, preservation and calcification in sediments from ODP Site 1263 (Walvis Ridge — SW Atlantic). Mar. Micropaleontol. 69, 119–138.
Ravani, A., Malinverno, E., Karatsolis, B-Th., Lagaria, A., Dimiza, M.D., Psarra, S., Triantaphyllou, M.V., 2017. Coccolithophore distribution in the western Black Sea during early summer 2016. J. Nannoplankt. Res. Abstr. 37 (INA16), 138–139.
Romanski, J., Romanou, A., Bauer, M., Tselioudis, G., 2012. Atmospheric forcing of the Eastern Mediterranean Transient by midlatitude cyclones. Geophys. Res. Lett. 39, L03703. https://doi.org/10.1029/2011GL050298.
Rost, B., Riebesell, U., 2004. Coccolithophores and the biological pump: Responses to environmental changes. In: Thierstein, H.R., Young, J.R. (Eds.), Coccolithophores from Molecular Processes to Global Impact. Springer, Berlin, pp. 99–125.
Roussakis, G., Karageorgis, A.P., Conispoliatis, N., Lykousis, V., 2004. Last glacial-Holocene sediment sequences in N. Aegean basins: structure, accumulation rates and clay mineral distribution. Geo-Mar. Lett. 24, 97–111.
Saavedra-Pellitero, M., Baumann, K.-H., 2015. Comparison of living and surface sediment coccolithophore assemblages in the Pacific sector of the Southern Ocean. Micropaleontology 61 (6), 507–520.
Samtleben, C., Schäfer, P., Andruleit, H., Baumann, K.-H., Baumann, A., Kohly, A., Matthiessen, J., Schroeder-Ritzrau, A., 1995. Plankton in the Norwegian- Greenland Sea: from living communities to Sediment Assemblages - an actualistic approach. Geol. Rundsch. 84, 108–136.
Souvermezoglou, E., Krasakopoulou, E., 2002. High oxygen consumption rates in the deep layers of the north Aegean Sea E. Mediterranean Mar. Sci. 3 (1), 55–65.
Souvermezoglou, E., Krasakopoulou, E., Pavlidou, A., 2014. Temporal and spatial variability of nutrients and oxygen in the North Aegean Sea during the last thirty years. Mediterr. Mar. Sci. 15, 805–822.
Stavrakakis, S., Chronis, G., Tselepides, A., Heussner, S., Monaco, A., Abassi, A., 2000. Downward fluxes of settling particles in the deep Cretan Sea (NE Mediterranean). Prog. Oceanogr. 46, 217–240.
Stavrakakis, S., Gogou, A., Krasakopoulou, E., Karageorgis, A.P., Kontoyiannis, H., Rousakis, G., Velaoras, D., Perivoliotis, L., Kambouri, G., Stavrakaki, I., Lykousis, V., 2013. Downward fluxes of sinking particulate matter in the deep Ionian Sea (NESTOR site), Eastern Mediterranean: seasonal and interranual variability. Biogeosci. Discuss. 10, 591–641.
Stothers, R.B., 1984. The Great Tambora eruption in 1815 and its aftermath. Science 224, 1191–1198.
Theocharis, A., Nittis, K., Kontoyiannis, H., Papageorgiou, M., Balopoulos, E., 1999. Climatic changes in the Aegean Sea influence the Eastern Mediterranean thermohaline circulation (1986–1997). Geophys. Res. Lett. 26, 1617–1620.
Theocharis, A., Krokos, G., Velaoras, D., Korres, G., 2014. An Internal Mechanism Driving the Alternation of the Eastern Mediterranean Dense/Deep Water Sources. In: Borzelli, G.L.E., Gacic, M., Lionello, P., Malanotte-Rizzoli, P. (Eds.), The Mediterranean Sea: Temporal Variability and Spatial Patterns, AGU Geophysical Monograph Series, 202. John Wiley & Sons. Inc., Oxford, U.K, pp. 113–137.
Triantaphyllou, M.V., Dermitzakis, M.D., Dimiza, M., 2002. Holo- and Heterococcolithophores (calcareous nannoplankton) in the gulf of Korthi (Andros island, Aegean Sea, Greece) during late summer 2001. Rev. Paleobiol. 21 (1), 353–369.
Triantaphyllou, M.V., Ziveri, P., Tselepides, A., 2004. Coccolithophore export production and response to seasonal surface water variability in the oligotrophic Cretan Sea (NE Mediterranean). Micropaleontology 50, 127–144.
Triantaphyllou, M.V., Ziveri, P., Gogou, A., Marino, G., Lykousis, V., Bouloubassi, I., Emeis, K.C., Kouli, K., Dimiza, M., Rosell-Mele, A., Papanikolaou, M., Katsouras, G., Nunez, N., 2009. Late Glacial-Holocene climate variability at the south-eastern margin of the Aegean Sea. Mar. Geol. 266, 182–197.
Triantaphyllou, M., Dimiza, M., Krasakopoulou, E., Malinverno, E., Lianou, V., Souvermezoglou, E., 2010. Seasonal variation in *Emiliania huxleyi* coccolith morphology and calcification in the Aegean Sea (Eastern Mediterranean). Geobios 43, 99–110.
Triantaphyllou, M.V., Gogou, A., Bouloubassi, I., Dimiza, M., Kouli, K., Rousakis, G., Kotthoff, U., Emeis, K.C., Papanikolaou, M., Athanasiou, M., Parinos, C., Ioakim, C.,

Lykousis, V., 2014. Evidence for a warm and humid Mid-Holocene episode in the Aegean and northern Levantine Seas (Greece, NE Mediterranean). Reg. Environ. Change 14, 1697–1712.
Velaoras, D., Lascaratos, A., 2010. North-Central Aegean Sea surface and intermediate water masses and their role in triggering the Eastern Mediterranean Transient. J. Mar. Syst. 83, 58–66.
Velaoras, D., Kassis, D., Perivoliotis, L., Pagonis, P., Hondronasios, A., Nittis, K., 2013. Temperature and salinity variability in the Greek seas based on POSEIDON stations time series: preliminary results. Mediterr. Mar. Sci. 14, 5–18.
Velaoras, D., Papadopoulos, V.P., Kontoyiannis, H., Papageorgiou, D., Pavlidou, A., 2017. The response of the Aegean Sea (Eastern Mediterranean) to the Extreme 2016–2017 Winter. Geophys. Res. Lett. 44. https://doi.org/10.1002/2017GL074761.
Wagner, S., Zorita, E., 2005. The influence of volcanic, solar and CO_2 forcing on the temperatures in the Dalton Minimum (1790–1830): a model study. Clim. Dyn. 25, 205–218.
Westbroek, P., Brown, C.W., Van Bleijswijk, J., Brownlee, C., Brummer, G.J., Conte, M., Egge, J., Fernandez, E., Jordan, R., Knappertsbusch, M., Stefels, J., Veldhuis, M., van der Wal, P., Young, J.R., 1993. A model system approach to biological climate forcing: the example of *Emiliania huxleyi*. Glob. Planet. Chang. 8, 27–46.
Winter, A., Jordan, R.W., Roth, P.H., 1994. Biogeography of living Coccolithophores in ocean waters. In: Winter, A., Siesser, W.G. (Eds.), Coccolithophores. Cambridge University Press, Cambridge, UK, pp. 161–178.
Young, J.R., Poulton, A.J., Tyrrell, T., 2014. Morphology of *Emiliania huxleyi* coccoliths on the northwestern European shelf – is there an influence of carbonate chemistry? Biogeosciences 11, 4771–4782.
Zervakis, V., Georgopoulos, D., Drakopoulos, P.G., 2000. The role of the North Aegean in triggering the recent Eastern Mediterranean climatic changes. J. Geophys. Res. 105 (C11), 26,103–26,116.
Zervakis, V., Georgopoulos, D., Karageorgis, A.P., Theocharis, A., 2004. On the response of the Aegean Sea to climatic variability: a review. Int. J. Climatol. 24, 1845–1858.
Zervoudaki, S., Christou, E.D., Assimakopoulou, G., Örek, H., Gucu, A.C., Giannakourou, A., Pitta, P., Terbiyik, T., Yöcel, N., Moutsopoulos, T., Pagou, K., Psarra, S., Ozsoy, E., Papathanassiou, E., 2011. Composition, production and grazing of copepods in the Turkish Straits System and the adjacent northern Aegean Sea during spring. J. Mar. Syst. 86, 45–56.
Ziveri, P., Young, J.R., Van Hinte, J.E., 1999. Coccolithophore export production and accumulation rates, In: On determination of sediment accumulation rates. GeoResearch Forum 5, 41–56.